

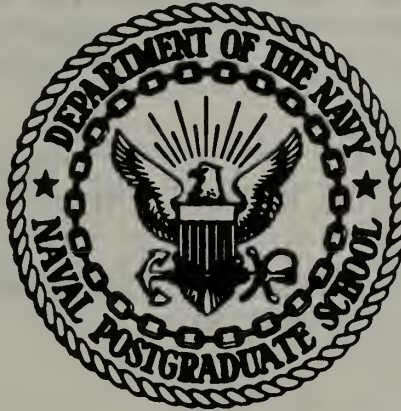
FINESTRUCTURE, FRONTS AND CURRENTS  
IN THE PACIFIC MARGINAL SEA-ICE ZONE -  
MIZPAC 78

Warren Edgar Small

DUDLEY KNOX LIBRARY  
NAVAL POSTGRADUATE SCHOOL  
MONTEREY, CA 93940

# NAVAL POSTGRADUATE SCHOOL

## Monterey, California



# THESIS

FINESTRUCTURE, FRONTS AND CURRENTS  
IN THE PACIFIC MARGINAL SEA-ICE ZONE -  
MIZPAC 78

by

Warren Edgar Small

June 1979

Thesis Advisors:

R. G. Paquette  
R. H. Bourke

Approved for public release; distribution unlimited.

A report submitted to:  
Director, Arctic Submarine Laboratory  
Naval Ocean Systems Center, San Diego, CA

T188664

NAVAL POSTGRADUATE SCHOOL  
Monterey, California

Rear Admiral T. F. Dedman  
Superintendent

Jack R. Borsting  
Provost

This thesis is prepared in conjunction with research supported in part by the Arctic Submarine Laboratory, Naval Ocean Systems Center, San Diego, California under Project Order Nos. 00002 and 00004.

Reproduction of all or part of this report is authorized.

Released as a Technical Report by:

Unclassified

SECURITY CLASSIFICATION OF THIS PAGE (When Data Entered)

## REPORT DOCUMENTATION PAGE

READ INSTRUCTIONS  
BEFORE COMPLETING FORM

1. REPORT NUMBER

NPS 68-79-002

2. GOVT ACCESSION NO.

3. RECIPIENT'S CATALOG NUMBER

4. TITLE (and Subtitle)

Finestructure, Fronts and Currents in the  
Pacific Sea-Ice Zone - MIZPAC 78

5. TYPE OF REPORT &amp; PERIOD COVERED

Interim  
14 Jul 78 - 12 Apr 79

6. PERFORMING ORG. REPORT NUMBER

NPS 68-78-002

7. AUTHOR(s)

Warren E. Small in conjunction with  
Robert G. Paquette and Robert H. Bourke

8. CONTRACT OR GRANT NUMBER(s)

N66001-78-P0-00002  
N66001-79-P0-00004

9. PERFORMING ORGANIZATION NAME AND ADDRESS

Naval Postgraduate School  
Monterey, California 9394010. PROGRAM ELEMENT, PROJECT, TASK  
AREA & WORK UNIT NUMBERSElement: 62759N; Work:  
MR01549A09; Project:  
ZF52-555; Task: ZF52-

11. CONTROLLING OFFICE NAME AND ADDRESS

Arctic Submarine Laboratory  
Code 54, Bldg. 371, Naval Ocean Systems  
Center, San Diego, CA 92152

12. REPORT DATE

555-001

June 1979

13. NUMBER OF PAGES

83

14. MONITORING AGENCY NAME &amp; ADDRESS (if different from Controlling Office)

15. SECURITY CLASS. (of this report)

Unclassified

15a. DECLASSIFICATION/DOWNGRADING  
SCHEDULE

16. DISTRIBUTION STATEMENT (of this Report)

Approved for public release; distribution unlimited.

17. DISTRIBUTION STATEMENT (of the abstract entered in Block 20, if different from Report)

18. SUPPLEMENTARY NOTES

19. KEY WORDS (Continue on reverse side if necessary and identify by block number)

Marginal Sea-Ice Zone, MIZPAC, CTD, thermal finestructure,  
Chukchi Sea, Arctic Ocean, oceanography, fronts, currents,  
salinity spiking.

20. ABSTRACT (Continue on reverse side if necessary and identify by block number)

Sharp vertical temperature fronts, complex temperature inversions and current patterns in the Chukchi Sea during MIZPAC 78 in July 1978 were investigated in a further effort to define the mechanisms for the formation and distribution of finestructure. In conformity with previous findings, upper and lower-layer fronts near the ice tended to be coincident in the V-shaped zones between bifurcating current streams; such fronts were not associated with

Unclassified

SECURITY CLASSIFICATION OF THIS PAGE (When Data Entered)





Unclassified

SECURITY CLASSIFICATION OF THIS PAGE(When Data Entered)

significant finestructure. Previous thought would indicate that finestructure is found near wedge-like fronts. However, the situations for which this could be tested in 1978 were too few to be conclusive.

Two of the principal ice embayments, which were apparently caused by warm water streams, were found in approximately the same locations as in previous years. Upper-level current streams, deduced from the ice melt-back into embayments and from warm-water cores, appear to be bathymetrically steered. Both of the above mentioned bays contain temperature finestructure. In the embayment north of Cape Lisburne the finestructure was fairly widely distributed in the southern half; in the embayment west of Pt. Barrow the finestructure was principally near the northern ice boundary. In the central Chukchi Sea some finestructure was found well south of the ice.

Unclassified

SECURITY CLASSIFICATION OF THIS PAGE(When Data Entered)





Approved for public release; distribution unlimited

Finestructure, Fronts and Currents  
in the Pacific Marginal Sea-Ice Zone -  
MIZPAC 78

by

Warren Edgar Small  
Lieutenant Commander, United States Navy  
B.S., Rensselaer Polytechnic Institute, 1969

Submitted in partial fulfillment of the  
requirements for the degree of

MASTER OF SCIENCE IN OCEANOGRAPHY

from the

NAVAL POSTGRADUATE SCHOOL  
June 1979



## ABSTRACT

Sharp vertical temperature fronts, complex temperature inversions and current patterns in the Chukchi Sea during MIZPAC 78 in July 1978 were investigated in a further effort to define the mechanisms for the formation and distribution of finestructure. In conformity with previous findings, upper and lower-layer fronts near the ice tended to be coincident in the V-shaped zones between bifurcating current streams; such fronts were not associated with significant finestructure. Previous thought would indicate that finestructure is found near wedge-like fronts. However, the situations for which this could be tested in 1978 were too few to be conclusive.

Two of the principal ice embayments, which were apparently caused by warm water streams, were found in approximately the same locations as in previous years. Upper-level current streams, deduced from the ice melt-back into embayments and from warm-water cores, appear to be bathymetrically steered. Both of the above mentioned bays contain temperature finestructure. In the embayment north of Cape Lisburne the finestructure was fairly widely distributed in the southern half; in the embayment west of Pt. Barrow the finestructure was principally near the northern ice boundary. In the central Chukchi Sea some finestructure was found well south of the ice.



## TABLE OF CONTENTS

I.	INTRODUCTION-----	10
A.	BACKGROUND-----	10
B.	MIZPAC 77-----	15
C.	MIZPAC 78-----	16
D.	OBJECTIVES-----	18
II.	EQUIPMENT AND TECHNIQUES-----	21
A.	CONDUCTIVITY-TEMPERATURE-DEPTH RECORDER (CTD)-----	21
B.	NANSEN CASTS-----	22
C.	CURRENT METER-----	23
D.	GAS SYRINGES-----	23
III.	DATA REDUCTION AND DISPLAY-----	24
A.	ERROR ANALYSIS AND CORRECTION-----	24
1.	Temperature-----	24
2.	Salinity-----	24
3.	Editing-----	25
4.	Despiking-----	28
B.	CALCULATIONS AND DISPLAY-----	28
1.	Sound Speed and Sigma-t-----	28
2.	Ice Edge-----	29
IV.	OCEANOGRAPHY OF THE MIZ-PREVIOUS OBSERVATIONS AND THEORIES-----	30
A.	WATER MASSES-----	30
1.	Northern Water-----	30
2.	Southern Water-----	32
3.	Transition Zone-----	34





B.	TEMPERATURE FRONTS-----	34
C.	FINESTRUCTURE-----	38
D.	INFERRED CURRENTS-----	45
1.	Ice Edge Recession-----	45
2.	Bathymetric Steering-----	47
V.	ANALYSIS-----	48
A.	CROSS-SECTIONS 2 AND 3-----	48
B.	CROSS-SECTIONS 4 AND 5-----	51
C.	THE WESTERN EMBAYMENT-----	56
D.	THE BARROW EMBAYMENT-----	62
E.	CROSS-SECTIONS 9 AND 10-----	66
F.	THE ICE "TONGUE"-----	69
VI.	CONCLUSIONS-----	74
	LIST OF REFERENCES-----	76
	INITIAL DISTRIBUTION LIST-----	78



## LIST OF TABLES

TABLE I.	MIZPAC 78 CRUISE SUMMARY-----	19
TABLE II.	ERROR ANALYSIS SUMMARY-----	26
TABLE III.	MIZPAC 78 FINESTRUCTURE CLASSIFICATION SYSTEM----	40
TABLE IV.	DISTRIBUTION AND INTENSITY OF FINESTRUCTURE - MIZPAC 78-----	42



## LIST OF FIGURES

Figure 1.	Property profiles for a station showing strong finestructure-----	11
Figure 2.	MIZPAC 78 station plot-----	17
Figure 3.	Property profiles of a representative station in the northern area -----	31
Figure 4.	Temperature and salinity cross-section No. 1-----	33
Figure 5.	Property profiles of a representative station in the southern area-----	35
Figure 6.	Nested temperature profile No. 1-----	36
Figure 7.	Nested temperature profile No. 2-----	39
Figure 8.	Distribution and intensity of finestructure during MIZPAC 78-----	41
Figure 9.	Upper level currents in the Chukchi Sea as inferred from gross ice edge recession rates from 17 to 25 July 1978 and bottom bathymetry----	46
Figure 10.	Temperature and salinity cross-section No. 2-----	49
Figure 11.	Temperature and salinity cross-section No. 3-----	50
Figure 12.	Temperature and salinity cross-section No. 4-----	52
Figure 13.	Temperature and salinity cross-section No. 5-----	53
Figure 14.	Nested temperature profile No. 3-----	54
Figure 15.	Temperature and salinity cross-section No. 5A----	57
Figure 16.	Temperature and salinity cross-section No. 6-----	59
Figure 17.	Temperature and salinity cross-section No. 7-----	60
Figure 18.	Temperature and salinity cross-section No. 8-----	61
Figure 19.	Temperature and salinity cross-section No. 11----	64
Figure 20.	Isotherms of maximum temperature in the water column for MIZPAC 78-----	65
Figure 21.	Temperature and salinity cross-section No. 9-----	67





Figure 22. Temperature and salinity cross-section No. 10----68

Figure 23. Temperature and salinity cross-section No. 12----70

Figure 24. Temperature and salinity cross-section No. 14----71

Figure 25. Temperature and salinity cross-section No. 13----72



## ACKNOWLEDGEMENT

I wish to express my gratitude to the faculty and staff of the Naval Postgraduate School for their help and guidance throughout my graduate studies. I am especially grateful to Drs. R. G. Paquette and R. H. Bourke. Their interest and patience were invaluable in the preparation of this thesis.



## I. INTRODUCTION

### A. BACKGROUND

Oceanographic investigations of the marginal sea-ice zone Pacific (MIZPAC) in the Chukchi Sea during the melt season have consistently uncovered phenomena which significantly deteriorate the propagation of underwater sound. Specifically, these include temperature fronts with horizontal gradients as large as  $2^{\circ}\text{C}/\text{km}$  and temperature finestructure with peak-to-peak fluctuations often exceeding  $2^{\circ}\text{C}$ . The operational significance of the effects of these phenomena is readily apparent upon viewing the sound velocity (SV) profile in Figure 1. Yet, it was over twenty years after the NEREUS recorded the first observations of finestructure in 1947 that the Arctic Submarine Laboratory, Naval Ocean Systems Center, San Diego, California, established PROJECT MIZPAC to investigate these phenomena. The chartered purpose of this project was to develop arctic submarine technology and to increase the understanding of the associated complex sound speed profiles and the inherent changes in propagation conditions both temporally and spatially in the marginal sea-ice zone (MIZ).

There have been six MIZPAC cruises conducted by the Naval Postgraduate School (NPS) since the first venture in 1971. The investigation of oceanographic processes responsible for the complex temperature and salinity structure near the ice margin in the Chukchi Sea has been the object of these cruises.





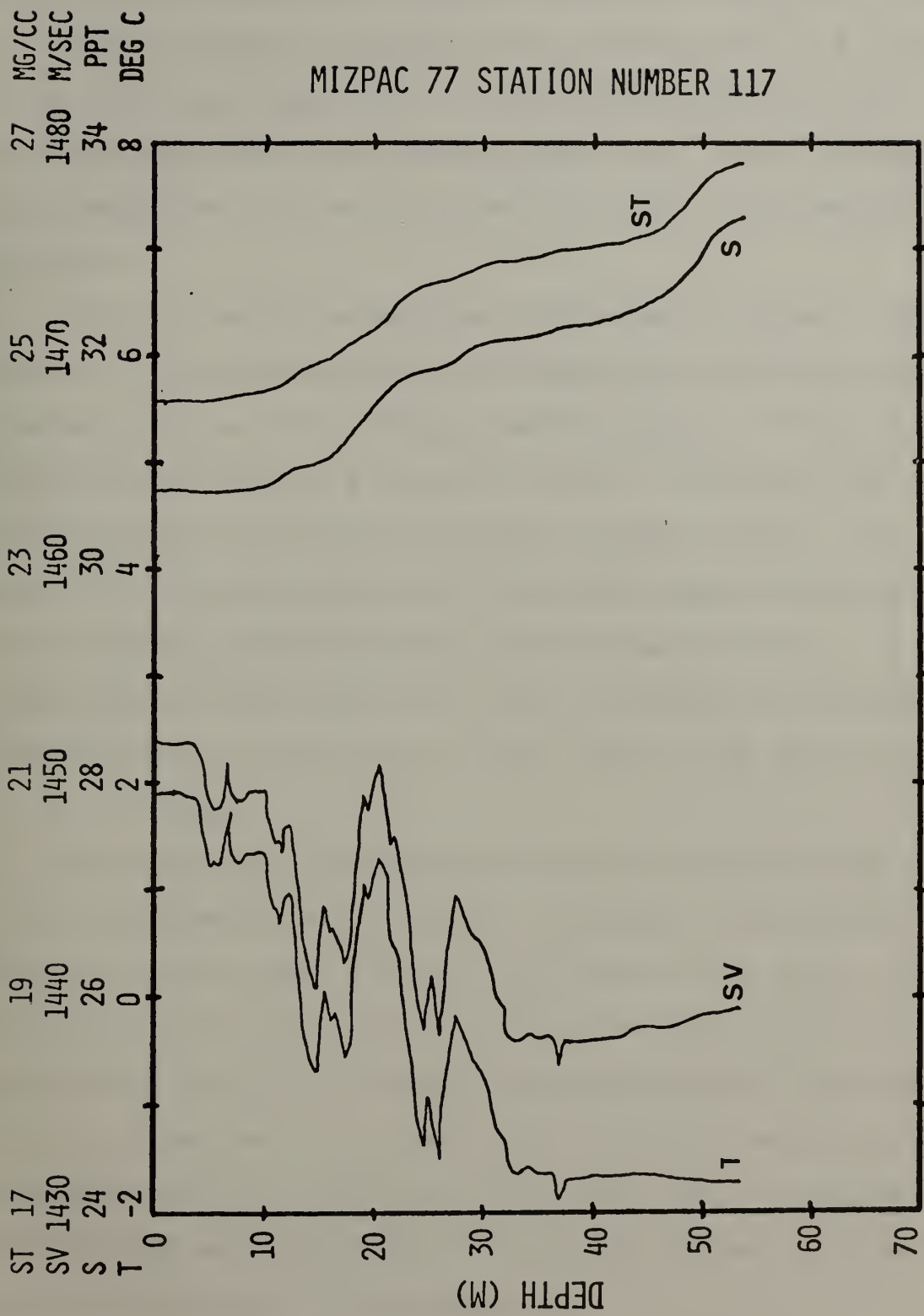


Figure 1. Property profiles for a station showing strong finestructure (after Graham, 1978).



Additionally, the later cruises, especially MIZPAC 78, sought to correlate earlier findings with processes that are still occurring on an annual cycle and validate hypotheses and predictions based upon this growing data bank. These hypotheses and predictions will be discussed in detail in subsequent sections.

MIZPAC 71 and 72 results were reported by Paquette and Bourke (1973) who described the temperature structure and fluctuations near the ice edge and the nature of the two-layered water structure south of the ice. Paquette and Bourke (1974) discussed the Alaskan Coastal Current, the descent of its warm water into mid-depth along the continental slope, and its eventual entry into the Beaufort Sea. It is significant to note that as a result of these two cruises, finestructure was believed to exist only in the near vicinity of the ice edge.

The space-time distribution of finestructure during MIZPAC 71 was examined by Corse (1974). He found a correlation between finestructure elements in a time-series over a period of several hours, but poor spatial correlation over distances as short as 1 km. The concept of finestructure formation due to the interaction of northward flow with ice keels causing a downward mixing of warm surficial water was introduced in this work as was the possible correlation between internal waves and the type of finestructure.

Karrer (1975) examined data from MIZPAC 74. He made heat and ice-melt evaluations in the vicinity of the ice edge and hypothesized that the local dynamic height gradient near the



ice edge was a possible driving force for downward mixing. The MIZPAC 74 results were further examined by Paquette and Bourke (1976). They suggested that finestructure formation was due to a lateral mixing process in mid-depth between warmer southerly water and a cold under-ice water, both of nearly the same density. Uneven mixing and interleaving of water types were hypothesized to be due to complex lateral pressures near the ice and the association of strong finestructure with rapid melting and rapid flow of warm water toward the ice was reported. They suggested that the ice margin controlled the northward flow of water, i.e., the Bering Sea water appeared to move northward at about the same rate as the ice margin retreated.

The results of MIZPAC 75 were reported by Zuberbuhler and Roeder (1976). The lessons learned from the previous MIZPAC cruises were incorporated in the cruise plan and some basic hypotheses on the formation and distribution of finestructure were tested. Significant discoveries included the existence of strong temperature fronts at the ice edge, the formation of finestructure in regions far removed from the ice edge, the existence of two water masses lying side-by-side and not mixing, and lifetimes of finestructure zones in excess of two days. An attempt to associate finestructure with directly measured currents was made, but the conclusions developed are questionable due to the effects of the ship's magnetism on the compass in the current meter.

Handlers (1977) studied aspects of a melt water zone and the correlation of the water flow rate with the rate of ice





edge retreat. He suggested that the surface currents flow faster than the ice retreats during the summer in the eastern half of the Chukchi Sea.

Paquette and Bourke (1978b) summarized the knowledge gained during the MIZPAC 71, 72, 74 and 75 cruises. They described the Chukchi Sea as a relatively shallow body of water where the only significant topographic feature is the Barrow Canyon to the northeast. It will be later shown that the relatively small changes in bottom bathymetry appear to exert a strong influence on current direction. The ice edge recession rate was determined to be a function of the heat supplied by water flowing northward from Bering Strait and the ice embayment north of Cape Lisburne and off Point Barrow were linked to bifurcations of this current. The formation of temperature and salinity fronts in the upper layers of the water everywhere along the ice edge were discussed as were the lower-layer fronts in which most of the finestructure to date had been found. The concept of a coincident front where the upper and lower-layer fronts coincide was introduced as was its association with an area of relatively weak component of current flow toward the ice, i.e., a zone of current shear parallel to the ice edge. The distribution of finestructure in the MIZ was given a geographic definition relative to the ice edge., i.e., within 10 km of the ice edge, and the rapid dissipation of heat after penetrating the ice was given as a reason for the scarcity of finestructure behind the ice edge. The year-to-year variability in the distribution of finestructure was attributed to annual variations in local ice-melt conditions.



## B. MIZPAC 77

MIZPAC 77 took place in July and August, 1977. The primary objective of this cruise was to find and characterize fine-structure in the vertical temperature profiles and to discover its horizontal distribution and causes. The results of the cruise, as reported by Graham (1978), were strikingly similar to the results of previous MIZPAC cruises with respect to the location and intensity of finestructure and inferred current patterns. He was subsequently able to present theoretical conclusions that were significant in the formulation of the cruise plan for the subsequent MIZPAC cruise in 1978.

Considerable finestructure was discovered during the MIZPAC 77 cruise, some of it deeper than any previously seen (>50m). The most striking temperature fronts noted thus far were found at the ice edge. A strong vertical temperature front was found within 15 km of the one reported by Zuberbuhler and Roeder (1976). All finestructure found in MIZPAC 77 was observed in a transition zone between under-ice water and water from the south.

Upper level currents were inferred from the rate of recession of the ice edge in 1977 as well as the shape of the ice edge as reported in other MIZPAC cruises. The inferred current patterns were in general agreement with those previously published.

Graham (1978) further suggested a geographic distribution of finestructure and temperature fronts that was associated with the direction of warm upper level currents. A moderate



to strong component of flow toward the ice was coupled with extensive finestructure while a weak component showed little or no finestructure. The strong vertical temperature fronts were found at the ice edge where the inferred upper level currents bifurcated and left an area of slow ice recession between the two branches.

### C. MIZPAC 78

The MIZPAC 78 cruise took place aboard USCGC GLACIER from 14 to 28 July 1978. The objectives of the cruise were twofold. The primary objective was the continuation of the finding and characterization of finestructure in the vertical temperature profiles and the discovery of its horizontal distribution. The other objective was to test the Graham (1978) hypothesis concerning the geographical distribution of finestructure and temperature fronts and the inference of upper level currents from the ice edge recession rate.

The stations sampled during MIZPAC 78 are shown in Figure 2; an "H" before a station number indicates a station occupied by a hovering helicopter. The ice edge depicted in Figure 2 (and all other figures with an ice edge) is not synoptic, but is constructed from the position of the ice edge at the time a station was occupied within sight of or within radar range of the ice edge. Transects where cross sections of temperature and salinity have been constructed are indicated by the solid lines connecting stations and numbered sequentially while broken lines indicate stations





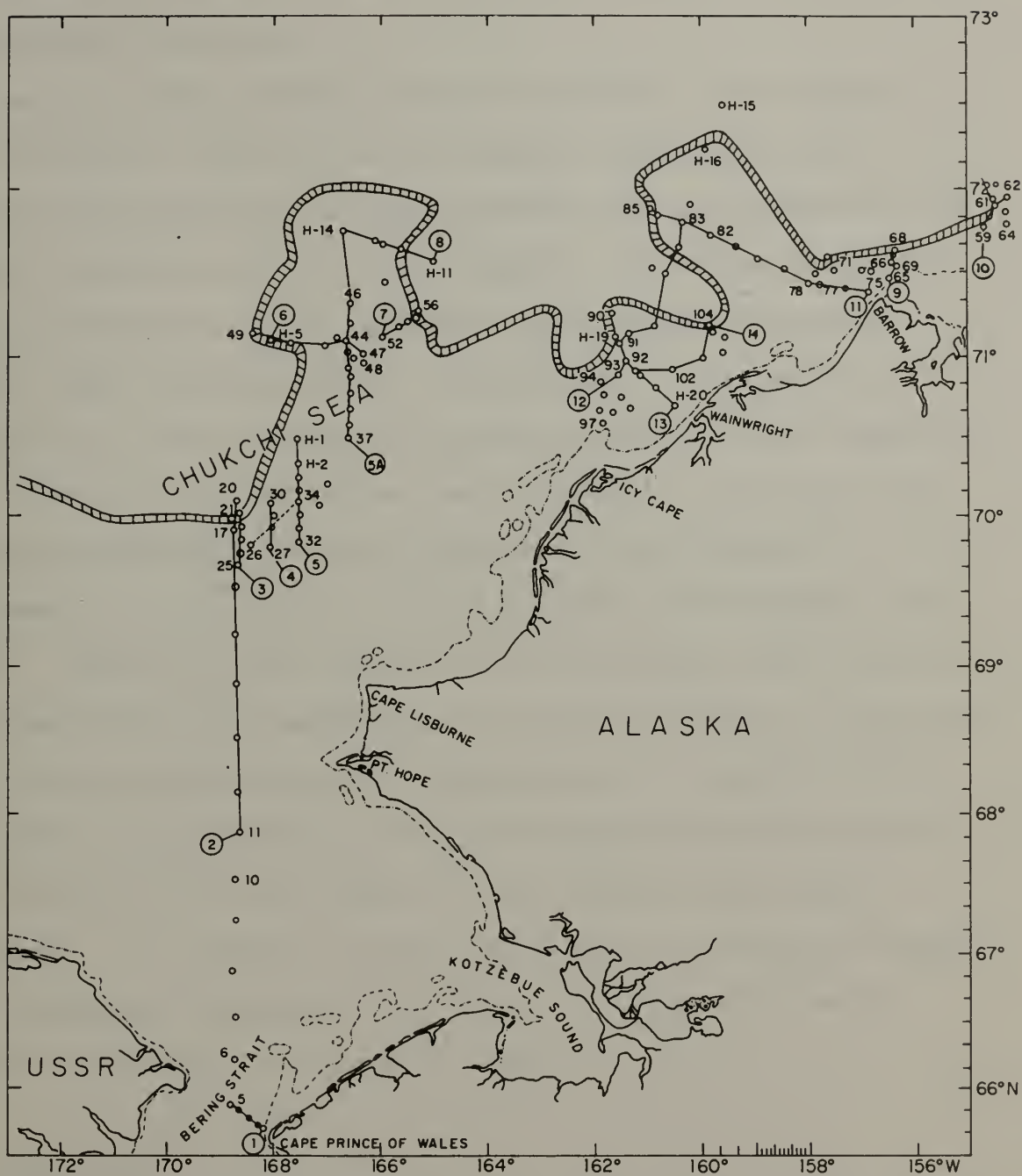


Figure 2. MIZPAC 78 station plot. The position of the ice edge at the time of each observation is also shown. The bold straight lines indicate positions of temperature-salinity cross-sections. Broken lines indicate nested temperature profiles.





for which nested temperature profiles have been drawn. Table I is a summary of some of the significant information pertaining to the MIZPAC 78 cruise.

Based on the previously stated objectives, the MIZPAC 78 cruise plan was laid out in two phases. The first part of the cruise investigated the central Chukchi Sea with concentration on the embayment north of Cape Lisburne. Stations were occupied in the center of the embayment as opposed to previous cruises when the majority of the stations were sampled in close proximity to the ice edge around the periphery of the embayment. The second part of the cruise was dedicated to investigating the eastern Chukchi Sea with emphasis on the embayment to the northwest of Point Barrow and the peculiar ice "tongue" found there. Temperature and salinity cross sections were constructed immediately upon completing a line of stations to determine the location and intensity of temperature or salinity fronts and afford an opportunity for reinvestigation of an area or for altering the cruise plan to investigate a particular phenomena. Ice margin crossings were made to localize temperature fronts and determine the extent of the projection of "under-ice" water from the ice margin.

#### D. OBJECTIVES

As was the case in previous MIZPAC cruises, considerable finestructure as well as several well-defined temperature fronts were discovered during the MIZPAC 78 cruises. This thesis will attempt to correlate the distribution and intensity



TABLE I  
MIZPAC 78 CRUISE SUMMARY

EMBARKATION:	14 July at Nome, Alaska
DEBARKATION:	28 July at Point Barrow, Alaska
OBSERVATION PLATFORMS:	USCGC GLACIER and her two helicopters
OCEANOGRAPHIC EQUIPMENT:	<ol style="list-style-type: none"> <li>1. Two lightweight CTD systems from the Applied Physics Laboratory, University of Washington.</li> <li>2. Nansen bottles and reversing thermometers.</li> <li>3. Pressure-Lok gas syringes.</li> </ol>
NAVIGATION SYSTEMS:	LORAN/Radar/OMEGA/Visual
STATIONS OCCUPIED:	130
STATIONS WITH USEFUL DATA:	128
NANSEN CASTS:	58
SCIENTIFIC PARTY:	<p>Dr. John Newton, NOSC, Chief Scientist</p> <p>Dr. Robert G. Paquette, NPS</p> <p>Dr. Robert H. Bourke, NPS</p> <p>LCDR Warren E. Small, USN, Student at NPS</p> <p>LT Walter R. Lohrmann, USN, Student at NPS</p> <p>LT Patricio Padilla, Ecuadorian Navy, Student at NPS</p>



of these phenomena and compare the results with previous years. Specifically, the results will be tested against the results of Graham (1978) and the association of current patterns, ice recession rates and the occurrence of fronts and finestructure will be further examined. This will be accomplished by examining areas investigated during MIZPAC 78 in light of the theories offered by Graham (1978) and Paquette and Bourke (1978 b and c). These areas include:

- the ice embayment north of Cape Lisburne
- the ice embayment northwest of Point Barrow
- the peculiar ice "tongue" to the south of this last embayment
- the regions of relatively slow ice edge recession
- the ice edge north of Point Barrow



## II. EQUIPMENT AND TECHNIQUES

### A. CONDUCTIVITY-TEMPERATURE-DEPTH RECORDER (CTD)

The primary data-gathering instrument during the MIZPAC 78 cruise was the hand-lowered CTD developed by the Applied Physics Laboratory, University of Washington (APL-UW) (Pederson, 1973). Data were recorded digitally on a cassette tape mounted on the winch drum. A lowering rate of approximately 1 m/sec was used, resulting in a data record rate of three points/m. Before leaving station, the CTD data were graphically plotted using a Hewlett-Packard 9100 series computer/plotter system. This technique enabled the watch team taking the measurements to ensure that good, usable data had been recorded. The plotted data afforded the scientists an opportunity to alter the proposed course of action to investigate a particular area or phenomena if necessary.

Twenty-four stations were occupied by lowering the CTD from a hovering helicopter. The same plotting procedure was followed as soon after the flight as possible. The utility of onboard plotting was shown when it was found by this technique that the CTD failed to function properly during two station lowerings on one flight. In all, 130 stations were occupied and usable data were recorded from 128 of them. Helicopter station locations were determined by fixing the ship's position at the time of the sampling and plotting a radar range and bearing to the hovering helicopter.







Both CTD's experienced equipment problems, with the replacement of several circuit boards becoming necessary before reliable operation could be expected. The malfunctions have been attributed to vibrations in several instances and a leaky cable in one other. The value of a sufficient supply of repair and replacement parts manifested itself during these situations.

After the cruise the cassette tapes were taken to APL-UW where the data were transferred to a seven-track tape and forwarded to NPS for editing and analysis.

#### B. NANSEN CASTS

Standardization of the CTD data was accomplished by comparing it with temperature and salinity data taken by reversing thermometers and Nansen bottles. A total of 58 casts were made with a Nansen bottle approximately 1 m above the sea floor. It was expected that this depth would place the bottle in a portion of the water column normally characterized by a uniform temperature and salinity profile. Forty-five samples were found to have been positioned in an isothermal layer and 38 in an isohaline layer. Positioning the bottle in such uniform layers was necessary to avoid errors due to depth uncertainties and non-simultaneity between the CTD and the Nansen bottle.



### C. CURRENT METER

In order to monitor the interchange of southern and northern bottom water near the ice edge, current speed and direction was to be measured with a current meter moored 2 m above the sea floor. An attempt at obtaining measurements was initiated, but extensive difficulties in maneuvering the icebreaker prevented further utilization of the current meter.

### D. GAS SYRINGES

MIZPAC 78 marked the first cruise that gas syringes were used to draw atmospheric and subsurface gas samples for future analysis ashore by gas chromatography techniques. The type of syringe used was the "Pressure-Lok Series A" gas syringe manufactured by the Precision Sampling Corporation. A total of 10 samples were taken at three separate stations and were analyzed through the courtesy of Dr. John Kelley of the Naval Arctic Research Laboratory for methane and carbon dioxide. The results were inconclusive; any further attempts to find correlations between these gases and water type or finestructure should be based on at least four times as many samples. Hence, the results will not be discussed in this report.



### III. DATA REDUCTION AND DISPLAY

#### A. ERROR ANALYSIS AND CORRECTION

##### 1. Temperature

The temperature of the water near the bottom was determined at 58 stations using standard reversing thermometers and these values were used as the standards for the temperature error analysis. CTD errors were plotted against time to find outliers and determine if there was a systematic drift. Fourteen outliers were identified and discarded. Further investigation revealed that most of these abnormalities were caused by excessive time delays between CTD lowerings and Nansen casts, probable equipment malfunctions, large temperature gradients over a small depth change, and excessive differences between sample depths for the CTD and Nansen casts. However, no systematic drift was found and the remaining 44 data points were used to calculate the statistics summarized in Table II. The raw CTD temperatures were subsequently corrected using the tabulated mean error correction.

##### 2. Salinity

The salinity of the bottom water at 51 stations was determined from the Nansen samples by means of a portable laboratory salinometer. As with temperatures, the CTD salinity errors were plotted against time to find outliers





and determine if there was a systematic drift. Ten outliers were found and discarded. The probable causes for these deviations were similar to those causing the deviations in the temperature recordings and resulted in a rapidly changing salinity reading with depth. Again, no systematic draft was found and the remaining 41 points were utilized in the calculation of the statistics presented in Table II. The salinity values, despiked as described in a following paragraph, were corrected using the tabulated mean error correction.

### 3. Editing

The CTD data contained erroneous values for a variety of reasons and were edited by Bourke and Paquette using a modified computer program, EDIT 4. The causes of error and their treatment are as follows:

- Salinity spikes due to a mismatch in conductivity and temperature response constants. These will be discussed in the next section.
- Anomalies produced when the lowering rate changed or reversed during the ship's rolling. These anomalies have their origin in the same instrumental causes as salinity spiking. Since the response constants of the sensors change with the rate of lowering, and the rate is continually varying in these cases, nice automatic correction is virtually impossible. We soon learned to lower





TABLE II  
MIZPAC 78 ERROR ANALYSIS SUMMARY

	<u>Temperature</u>	<u>Salinity</u>
NUMBER OF POINTS	44	41
MEAN ERROR CORRECTION (NANSEN-CTD)		
CTD #3	+0.012 <sup>o</sup> C	-0.007 <sup>o</sup> /oo
CTD #4	+0.045 <sup>o</sup> C	+0.007 <sup>o</sup> /oo
STANDARD DEVIATION		
CTD #3	±0.0140 <sup>o</sup> C	±0.0184 <sup>o</sup> /oo
CTD #4	±0.0358 <sup>o</sup> C	±0.0204 <sup>o</sup> /oo



faster when the ship rolled up and vice versa, which eased the difficulties somewhat. However, relatively few stations were so affected. The editing program contains a "ratchet" routine which rejects decreasing values of depth and interpolates for all the variables a number of points equal to the number of rejected points between the present accepted depth and the previous accepted depth. This accomplishes considerable rectification but unavoidably leaves some response error.

- Individual instrumental noise spikes. When these are single isolated spikes, they are easily removed by a routine called NOISE. However, if there are two or more points in the spike, the spike is not unambiguously distinguishable from a real spike, except that its magnitude may make it suspect. Such spikes were flagged for visual inspection and removed by other routines in the EDIT 4 program.
- Self-heating of the conductivity cell when it is motionless in the water. This phenomena occurred most often at the bottom and the aberrant data were removed manually.



#### 4. Despiking

Despiking was carried out by Professors Bourke and Paquette following principles outlined in their report (1978a). A correction based upon the slope of the conductivity curve was separated from that due to physical displacement of the sensors and digital sampling lag. This resulted in a somewhat more logical correlation procedure.

As was found previously, there is some subjectivity involved in assigning the constants for despiking which were found to vary somewhat from station to station. In several cases, it could be seen that perfect despiking was not possible by any choice of constants, which suggests that second or higher-order sensor responses are involved. Modeling such responses is not feasible at present. Therefore, it was necessary to smooth the despiked data with a running mean over five points. As a consequence of the subjectivity in choosing constants, it is not possible to certify that real salinity inversions, if such exist, have not been removed by despiking.

### B. CALCULATIONS AND DISPLAY

#### 1. Sound Speed and Sigma-t

Using the corrected values of salinity and temperature, values of sound speed and density (sigma-t) were calculated by computer. Plots of temperature, salinity, sound speed and sigma-t were subsequently produced and are included in a formal



technical report of MIZPAC 78 currently being published (Paquette and Bourke, in press). The temperature and salinity plots are the only results being utilized in this thesis.

## 2. Ice Edge

As was mentioned earlier, the ice edge depicted in Figures 2, 8, and 9 is not synoptic but rather the result of combining visual and radar observations of the ice margin while occupying stations in or near the ice. Gaps in the presentation of the location of the ice edge were filled in by plotting the ice edge as promulgated by the routine ice edge messages originated by the Fleet Weather Facility, Suitland, Maryland. This type of presentation is more useful than the synoptic in correlating station data with ice-related phenomena.





#### IV. OCEANOGRAPHY OF THE MIZ - PREVIOUS OBSERVATIONS AND THEORIES

##### A. WATER MASSES

The three areas described by Graham (1978) and modified slightly by Paquette and Bourke (1978b) will be used in subsequent discussions in this study. Two of the areas, defined as northern and southern waters, contain water with relatively consistent temperature and salinity values. The third area, called a transition area, lies between the other two and is characterized by a variety of temperature and salinity profiles.

##### 1. The Northern Water

The northern area water, referred to in the future as northern water, is found under the ice and generally within 20 km outward from the ice edge. A representative plot of the property profiles of a typical station occupied during MIZPAC 77 in northern water is shown in Figure 3. A sharp halocline extending anywhere from 2 to 18 m below the surface is found to normally divide the water of this area into two layers of sharply differing salinities.

The lower layer contains water of relatively high salinity, usually ranging from 32.8 to 33.5 ‰. The mean maximum salinity appears to vary from year to year, possibly due to changes in the rate of flow through Bering Strait and the amount of sea-ice formed (Paquette and Bourke, 1978b).



ST 17  
SV 1430  
S 24  
T 0

19  
1440  
26

21  
1450  
28

23  
1460  
30

25  
1470  
32

27  
1480  
34

MG/EC  
M/SEC  
P.D.T  
DEG C

# MIZPAC 77 STATION NUMBER 10H

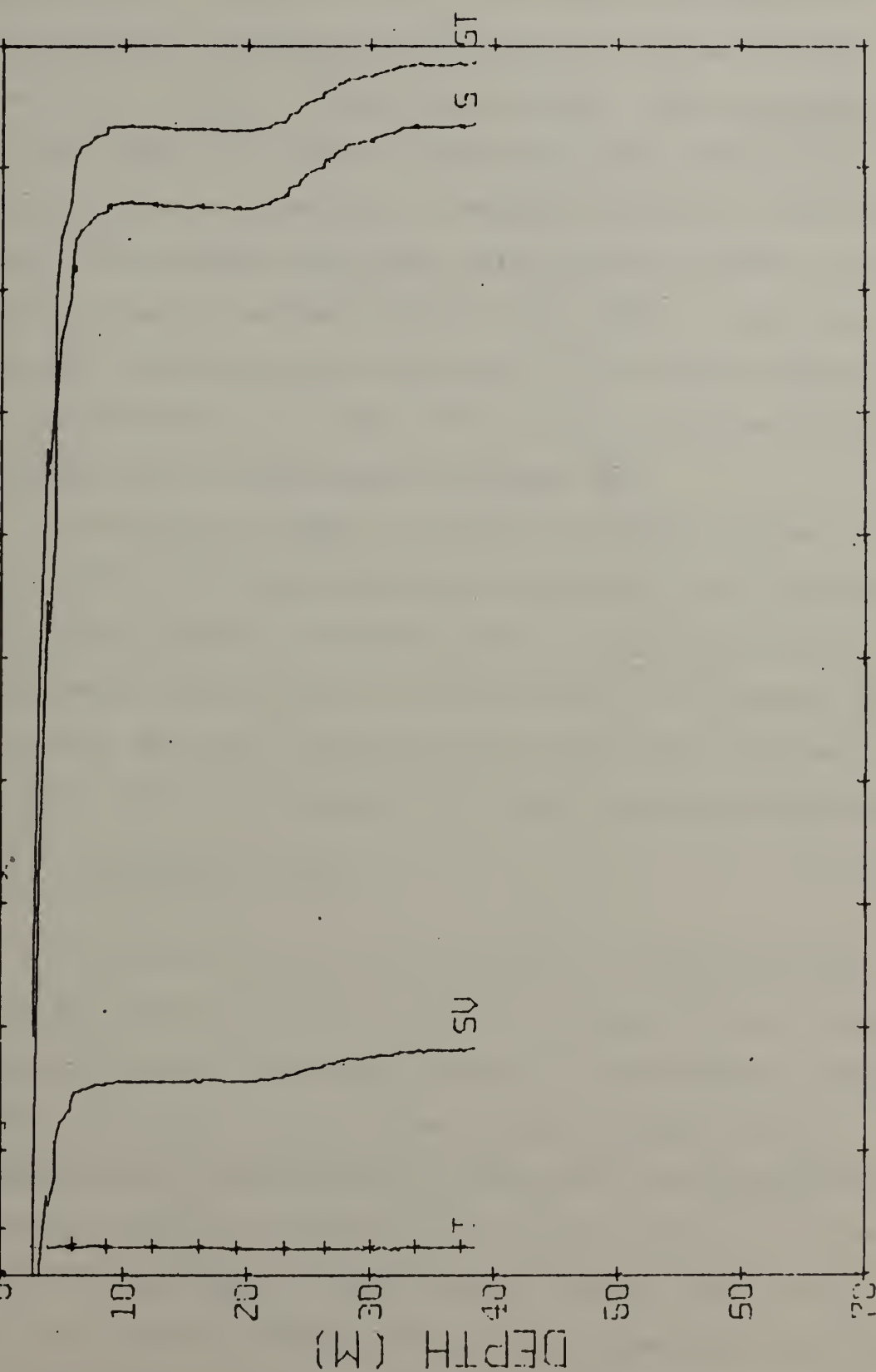


Figure 3. Property profiles of a representative station in the northern area (after Graham, 1978).



Water in this salinity range has an equilibrium freezing temperature of  $-1.6^{\circ}$  to  $-1.8^{\circ}\text{C}$ , i.e., the relationship of salinity to the freezing process prevents the water from becoming any colder. Paquette and Bourke (1976) suggested that this water is a relic of under-ice brine convection resulting from the freezing of seawater during the previous winter. They called this water, plus slightly warmed, slightly diluted products, northern bottom water (NBW). This year, water with salinities lower than  $32.8\text{ }^{\circ}/\text{oo}$  but with sufficiently cold temperature ( $-1.6^{\circ}$  and  $-1.7^{\circ}\text{C}$ ) to be considered NBW was found and will be considered as diluted NBW.

Overlying the NBW is a layer of slightly warmer ( $-1^{\circ}$  to  $0^{\circ}\text{C}$ ) and significantly less saline ( $\leq 28\text{ }^{\circ}/\text{oo}$ ) water. The property changes are clearly due to the effects of ice melting while the thickness of this layer is a function of the rate of melt and the speed of the upper layer current. This layer shall be referred to as upper-level northern water.

## 2. The Southern Water

The area in which southern water was found includes all of the Chukchi Sea from which all evidence of the ice and the northern water have been removed by warm currents and protracted insolation. As it flows through Bering Strait, southern water is only slightly stratified in temperature and virtually isohaline in salinity as noted in Figure 4. However, north of Bering Strait, in the central Chukchi Sea, these waters are found stratified strongly in temperature and weakly in salinity with the thermocline at an average depth of 5 to



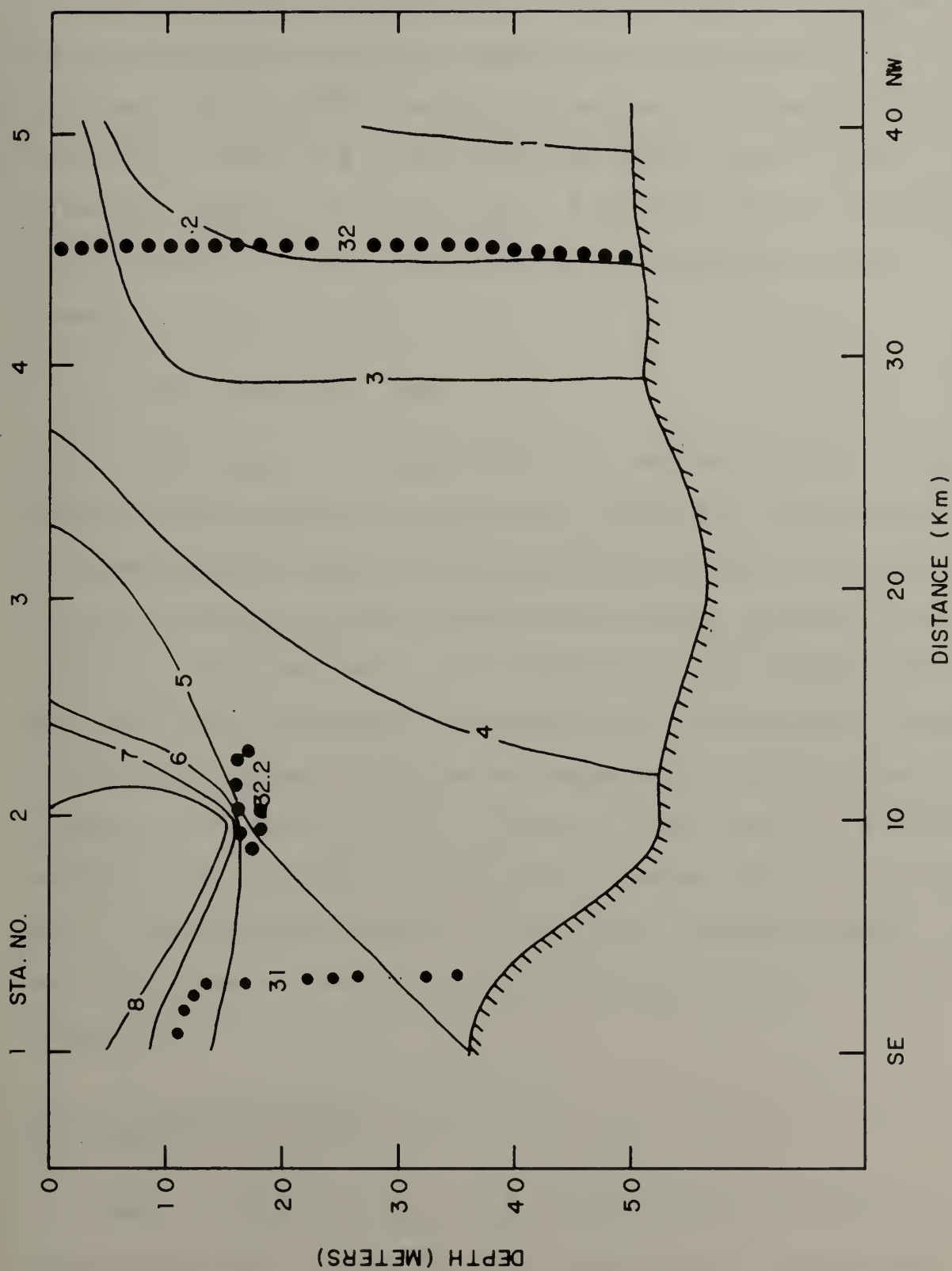


Figure 4. Temperature and salinity cross section No. 1.  
 Temperatures are in degrees centigrade ( $^{\circ}\text{C}$ ).  
 Salinities are in parts per thousand ( $^{\circ}/\text{oo}$ ).





20 m. The lower layer, termed southern bottom water (SBW), has temperatures varying between  $0^{\circ}$  and  $2^{\circ}\text{C}$  while the upper layer demonstrated maximum temperatures as high as  $9^{\circ}\text{C}$  in 1978 and  $10^{\circ}\text{C}$  in 1972. Salinities in the SBW generally vary between 32.2 and  $32.6 \text{ }^{\circ}/\text{oo}$ , while the upper layer is considerably fresher, 30 to  $32 \text{ }^{\circ}/\text{oo}$ . A representative station in the southern area is typified by the property profiles shown in Figure 5.

### 3. The Transition Zone

The transition zone waters lie between the well-defined northern and southern bottom waters. They are characterized by a progressive change in physical properties in a horizontal direction between the two bottom water masses discussed previously. Its dimensions vary considerably with widths extending from a few kilometers to as much as 125 km between the two bottom water masses. The nested temperature profile shown in Figure 6 illustrates how the transition zone water is gradually modified from the cold northern bottom water at Stations H-19 and 91 to the warmer water at Station 92. Another example, in which the zone is perhaps 70 to 140 km wide, may be seen in Figure 10.

#### B. TEMPERATURE FRONTS

Temperature fronts have been found during every MIZPAC cruise since 1975. In this thesis, two types of temperature fronts will be considered. First will be the upper-layer



ST SU S T  
 17 1430 24 2  
 19 1440 25 0  
 21 1450 28 7  
 23 1450 30 4  
 25 1470 32 5  
 27 1480 34 8  
 MS/CS  
 M/SEC  
 P.P.T.  
 DES C

# MIZPAC 77 STATION NUMBER

1

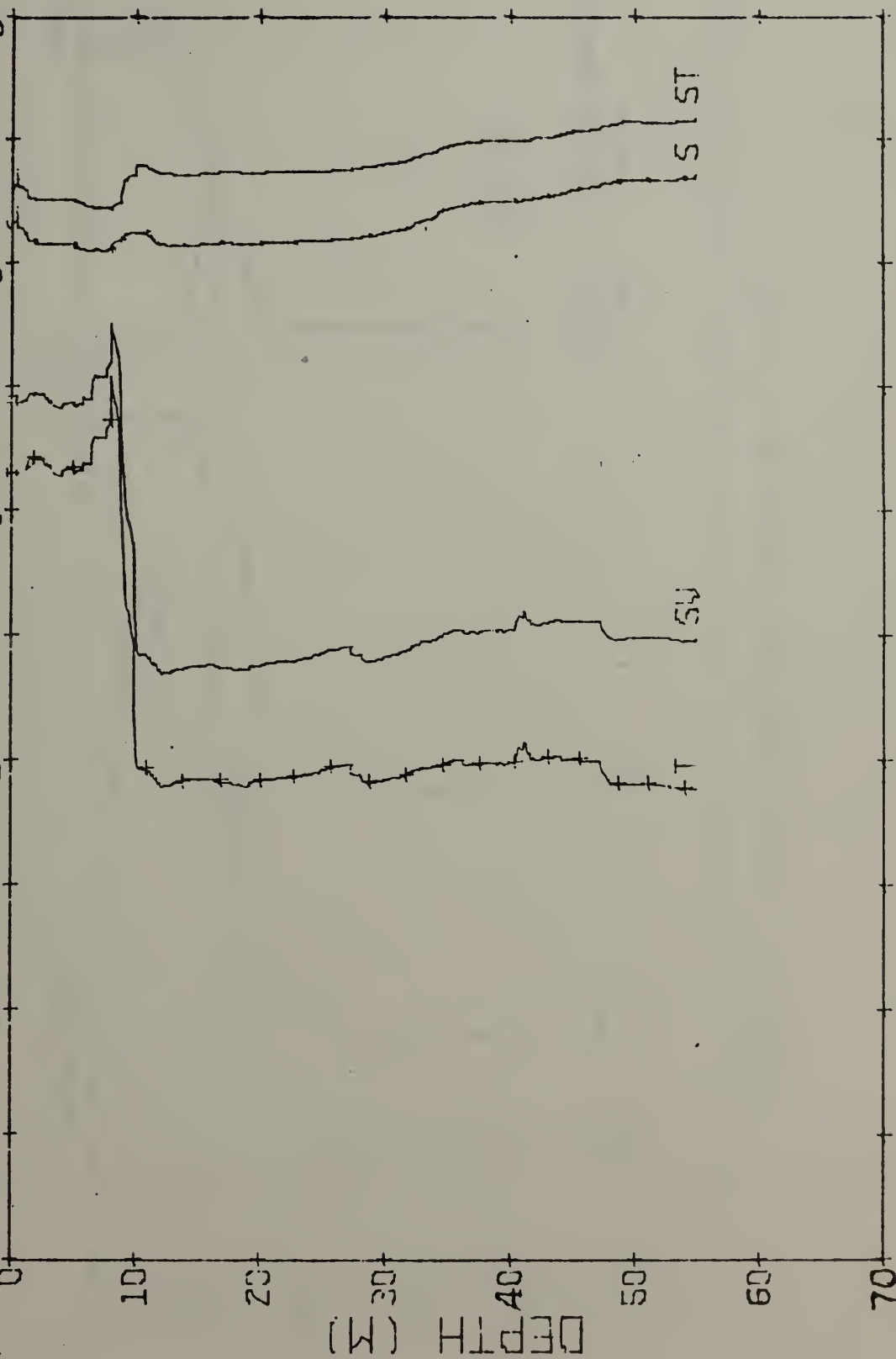


Figure 5. Property profiles of a representative station in the southern area (after Graham, 1978).



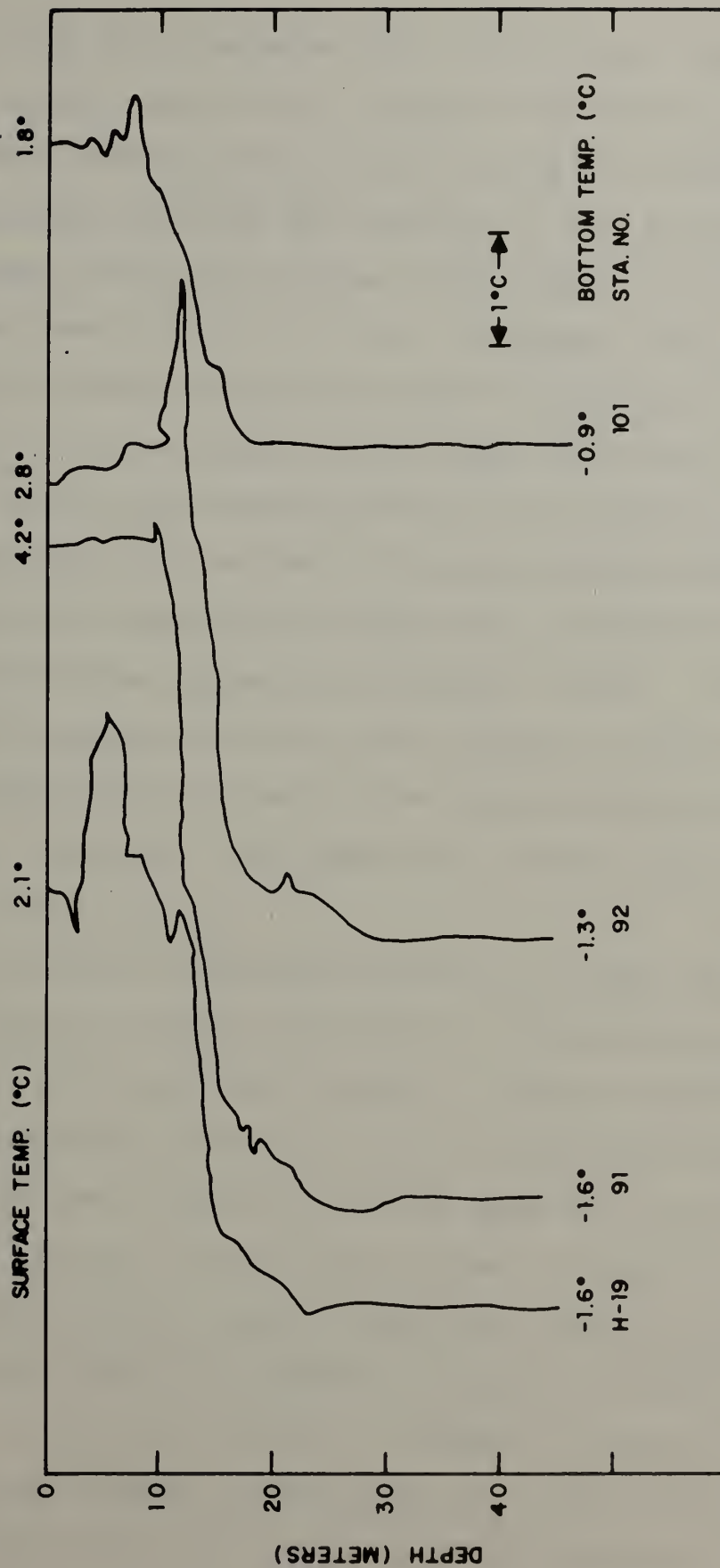


Figure 6. Nested temperature profile No. 1, 1978.





fronts which are associated with the melting of sea ice (this type of front usually has a salinity front associated with it). Upper layer fronts generally have strong horizontal gradients of temperature ( $2^{\circ}\text{C}/\text{km}$ ) and salinity ( $2\text{ }^{\circ}/\text{oo}$  per km). The upper-layer fronts encountered during MIZPAC 78 rarely extended deeper than 15 to 20 m. An example of an upper layer temperature front is seen in Figure 18 where the ice edge at Station H-12 is cooling the warm upper-layer water.

The lower-layer fronts examined were generally associated with the contact of northerly-flowing southern bottom water or transition water with the cold relic northern bottom water near the ice edge (Paquette and Bourke, 1978c). These fronts were quite complex in nature with respect to their location and strength and were found to be the area of most fine-structure formation. An example of a lower layer front is seen in Figure 10.

The horizontal separation between the upper and lower-layer fronts in the MIZ has been of considerable interest during the last two MIZPAC cruises. Paquette and Bourke (1978c) suggested the possibility of considerable distances between the two (as great as 70 km) generally in regions where the current flow is mainly normal to the ice edge. They further indicate that a wedge-like lower layer front exists where there is a moderate component of flow towards the ice. This type of front is somewhat irregular, but the northern and southern bottom waters are still well-defined and regions having such fronts seem to be areas of extensive finestructure formation. Both authors agreed with the



Graham (1978) prediction of coincident upper and lower-layer fronts in areas where there were weak components of current flow normal to the ice, particularly where the currents had bifurcated and the ice edge recession rate was relatively slow. Such an area is quiescent in the upper levels and the flow of southern water effectively shears off the northern bottom water that would normally protrude from the ice edge. Finestructure is not expected to be formed under these conditions and none has been observed in the immediate vicinity of coincident fronts. The fronts found during MIZPAC 78 will be examined in light of these suggestions in subsequent discussions.

### C. FINESTRUCTURE

Finestructure is characterized by large property inversions over a relatively small vertical distance. The property pertinent to this thesis is temperature, which has been found to have fluctuations as large as  $2^{\circ}\text{C}$  over a vertical extent of just a few meters. An example of a temperature profile exhibiting finestructure has already been shown in Figure 1 and may also be seen in Figure 7, Station 43. The classification scheme used to describe the intensity of finestructure in this thesis is displayed in Table III (after Paquette and Bourke, 1978b). The concept of a "nose," introduced by Paquette and Bourke (1978b), is included in this table. A chart illustrating the intensity and distribution of finestructure with respect to the ice edge during MIZPAC 78 is shown in Figure 8. Table IV summarizes this intensity and distribution.



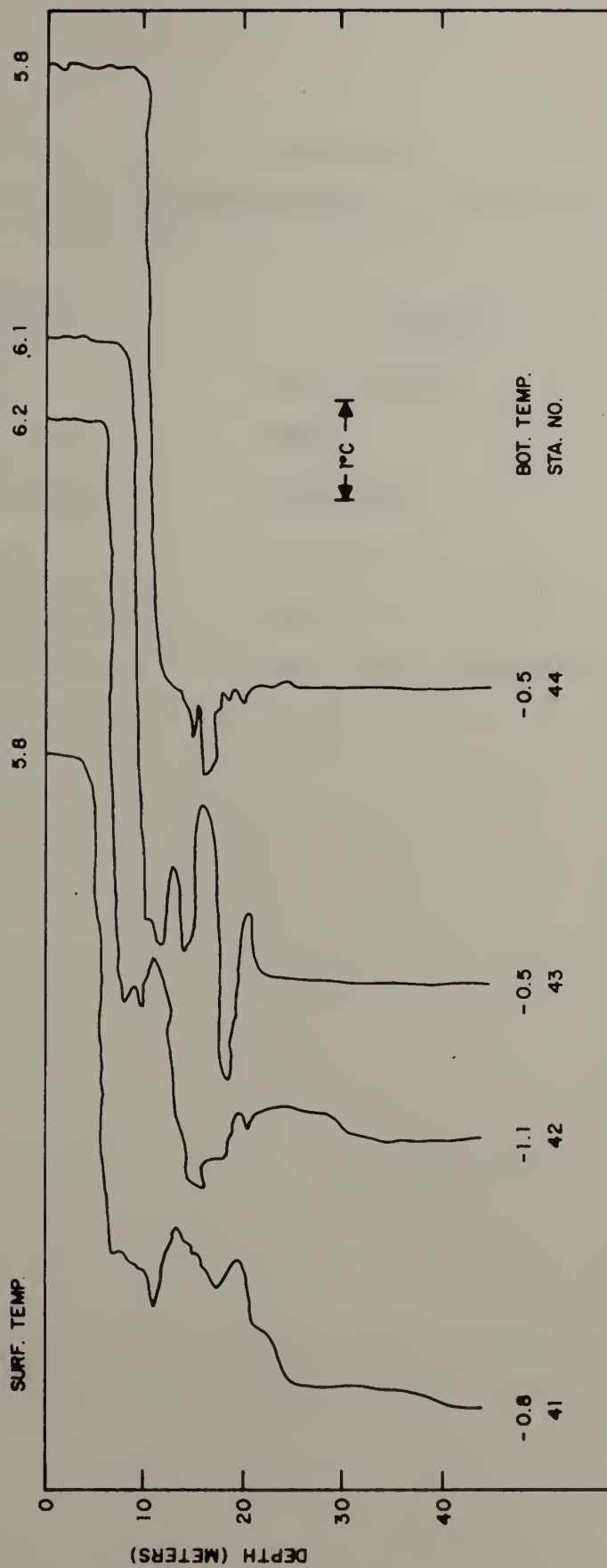


Figure 7. Nested temperature profile No. 2. Temperatures are in °C.



TABLE III  
MIZPAC 78 FINESTRUCTURE CLASSIFICATION SYSTEM

<u>Symbol</u>	<u>Category</u>	<u>Peak-to-Peak Fluctuation</u>
Open circle	Nonexistent	$<0.2^{\circ}\text{C}$
Circle with dot	Weak	0.2 to 0.5 deg C
Circle with cross	Moderate	0.5 to 1.0 deg C
Solid circle	Strong	More than 1.0 deg C
Open tab on circle	Nose w/o structure	
Solid tab on circle	Nose with structure	





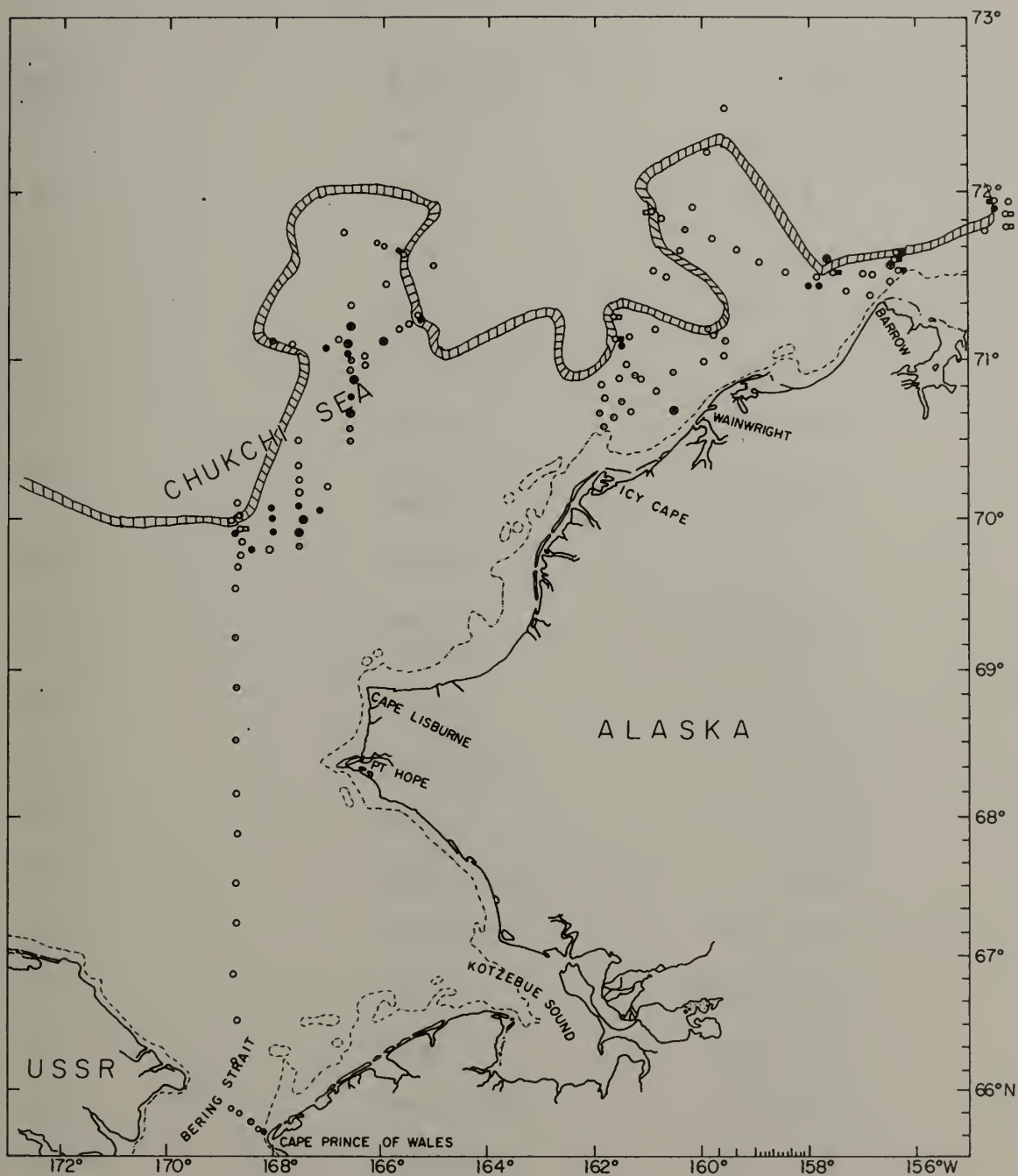


Figure 8. Distribution and intensity of finestructure during MIZPAC 78. Symbols are described in Table II. The ice edge is shown as the hatched line.



TABLE IV

## DISTRIBUTION AND INTENSITY OF FINESTRUCTURE - MIZPAC 78

<u>Station Number</u>	<u>Category</u>	<u>Depth</u>
003	Weak	09-14 m
013	Weak	38-44 m
014	Weak	27-27 m
015	Weak	20-24, 32-36 m
017	Strong	15-20 m
022	Nose	04-09 m
026	Strong Weak	10-13 m 31-39 m
028	Strong	08-18 m
029	Weak Strong	06-11 m 19-27 m
030	Strong	10-20 m
031	Moderate	25.32 m
032	Weak	15-25 m
033	Moderate	15-19 m
034	Strong	16-25 m
037	Weak	12-25 m
038	Weak	08-11 m
039	Moderate	08-21 m
040	Strong	07-14 m
041	Moderate	06-21 m
042	Weak	07-14 m
043	Strong	08-21 m



TABLE IV (Cont'd)

<u>Station Number</u>	<u>Category</u>	<u>Depth</u>
044	Moderate	16-19 m
045	Moderate	07-21 m
052	Moderate	24-28 m
056	Nose	01-08 m
060	Strong	05-32 m
061	Nose	05-15 m
	Moderate	85-90 m
063	Nose	02-09 m
064	Nose	03-09 m
066	Moderate	06-12 m
067	Nose	05-10 m
	Moderate	65-69 m
068	Nose	03-27 m
	Moderate	60-65 m
	Weak	87-90 m
069	Nose	15-20 m
071	Nose	04-09 m
	Moderate	09-15 m
072	Moderate	03-09, 16-25 m
077	Strong	07-18 m
	Weak	73-91 m
078	Strong	13-23 m
085	Nose	04-09 m
090	Nose	15-20 m
091	Strong	06-11 m
096	Weak	08-19 m
097	Weak	17-22 m
098	Weak	12-17 m





TABLE IV (Cont'd)

<u>Station Number</u>	<u>Category</u>	<u>Depth</u>
099	Weak	13-23 m
101	Weak	03-08 m
102	Weak	05-10, 19-22 m
104	Weak	08-11 m
106	Strong	06-20 m
H-4	Strong	19-25 m
H-7	Nose	03-08 m
	Strong	11-19 m
H-8	Weak	11-14 m
H-11	Weak	08-15 m
H-12	Weak	03-09 m
H-18	Weak	15-24 m
H-19	Nose	03-13 m
H-20	Moderate	12-20 m



The processes that foster finestructure formation near the MIZ have been discussed by Corse (1974), Karrer (1975), and Paquette and Bourke (1978b) and will not be covered in this discussion. Rather, the predictions of Graham (1978) will be examined in light of the data gathered during MIZPAC 78 (refer to Section IB). As each particular region is examined, the distribution with respect to inferred currents and the ice edge will be considered.

#### D. INFERRED CURRENTS

##### 1. Ice Edge Recession

Paquette and Bourke (1978b) indicated that the melting of the ice edge is concentrated at the line of contact of the northward-flowing southern water and the ice edge. This was expanded by Graham (1978) who associated the recession of the ice edge with a presumed iceward flow of the warm upper level currents since they were expected to carry most of the heat to the ice. By plotting the positions of the ice edge and their subsequent movements, he inferred the movement of currents as a function of ice edge recession. The resulting flow regime conformed well to the patterns postulated by Coachman et al. (1975). Figure 9 from MIZPAC 78 shows results closely corresponding to Graham's (1978) hypothesis. The upper level currents inferred from the cores of warm water correspond well with both Coachman et al. and Graham and also with the ice melt-back pattern.



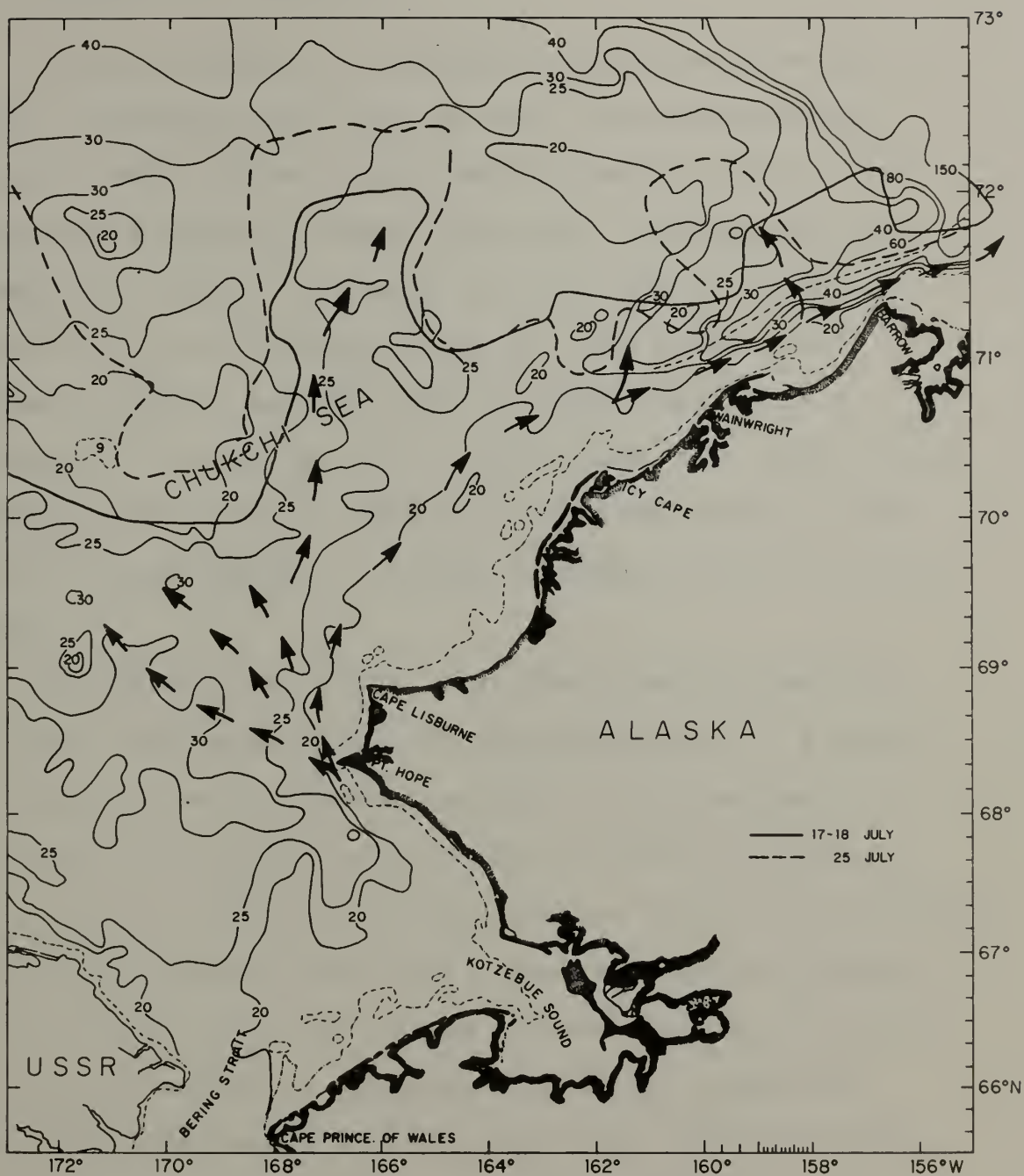


Figure 9. Upper level currents in the Chukchi Sea as inferred from gross ice edge recession rates from 17 to 25 July 1978, bottom bathymetry, and water column temperature maxima. Bottom contours are in fathoms. The dashed line paralleling the coast represents the 10 fathom curve.



## 2. Bathymetric Steering

Prior to MIZPAC 78, the MIZPAC researchers tended to consider the Chukchi Sea floor as flat and bathymetrically featureless with a more or less uniform depth of 50 m. An examination of Figure 9 reveals that this consideration is not completely valid. A change in depth of 5 to 10 fm over a distance of a few kilometers may not seem particularly important at first, but when such a change represents a variation of 10 to 20 per cent in the length of a water column containing vorticity, it takes on a new significance. The effects of these changes in bottom topography must be further examined.

Coachman et al. (1975) indicated that the upper and lower-level flow patterns in the Chukchi Sea are to a marked degree parallel to the bottom contours. The divergence of the 40 and 50 m contours north of Cape Lisburne (Coachman et al., 1975, p. 142) was coupled with the split of the current coming through Bering Strait and branching, following Herald Canyon to the west and the bottom contours leading to Barrow Canyon to the northeast. However, the writer tentatively assumes that bathymetric steering may take place on slopes tilting downward either to the left or right of the direction of flow and irrespective of the direction of the isobaths. The work of Johnson (1978) indicates that the effects of bathymetry may be complex and dependent on the magnitudes of several parameters. This concept of bathymetric steering will be applied to the currents believed to be causing the ice embayments discussed in subsequent sections.





## V. ANALYSIS

### A. CROSS-SECTIONS NOS. 2 AND 3

Figures 10 and 11 show a striking coincident temperature front that extends from the surface to the sea floor. In both cases it is almost precisely at the ice margin and evidently extends east-west at least the 4 km spacing between the two lines. A front of similar nature and intensity was found in the same general geographic location and ice edge setting during the MIZPAC 75 and 77 cruises.

Using the concepts of ice edge recession rate to infer upper-layer currents and the theory of bathymetric steering introduced earlier, we can see from Figure 9 that the location of the front depicted in Figures 10 and 11 is in a quiescent, semi-stagnant or vortical area of upper level flow. The flow regimes in the frontal areas of the 1975 and 1977 cruises were similar. The finding of a coincident temperature front in such a region tends to support Graham (1978) who predicted such fronts when the flow of southern water is weak and parallel to the ice edge.

Figure 10 shows  $-1.7^{\circ}\text{C}$  water associated with a salinity of  $32.6\text{ }^{\circ}/\text{oo}$  at Station 20. Although this is a rather low salinity for NBW, it is assumed that higher salinities would be present farther north into the ice. Figure 11 shows the same general area revisited almost 12 hours later. Here we find the high salinity ( $32.8\text{ }^{\circ}/\text{oo}$ ) water at Station 21, somewhat further south than Station 20.



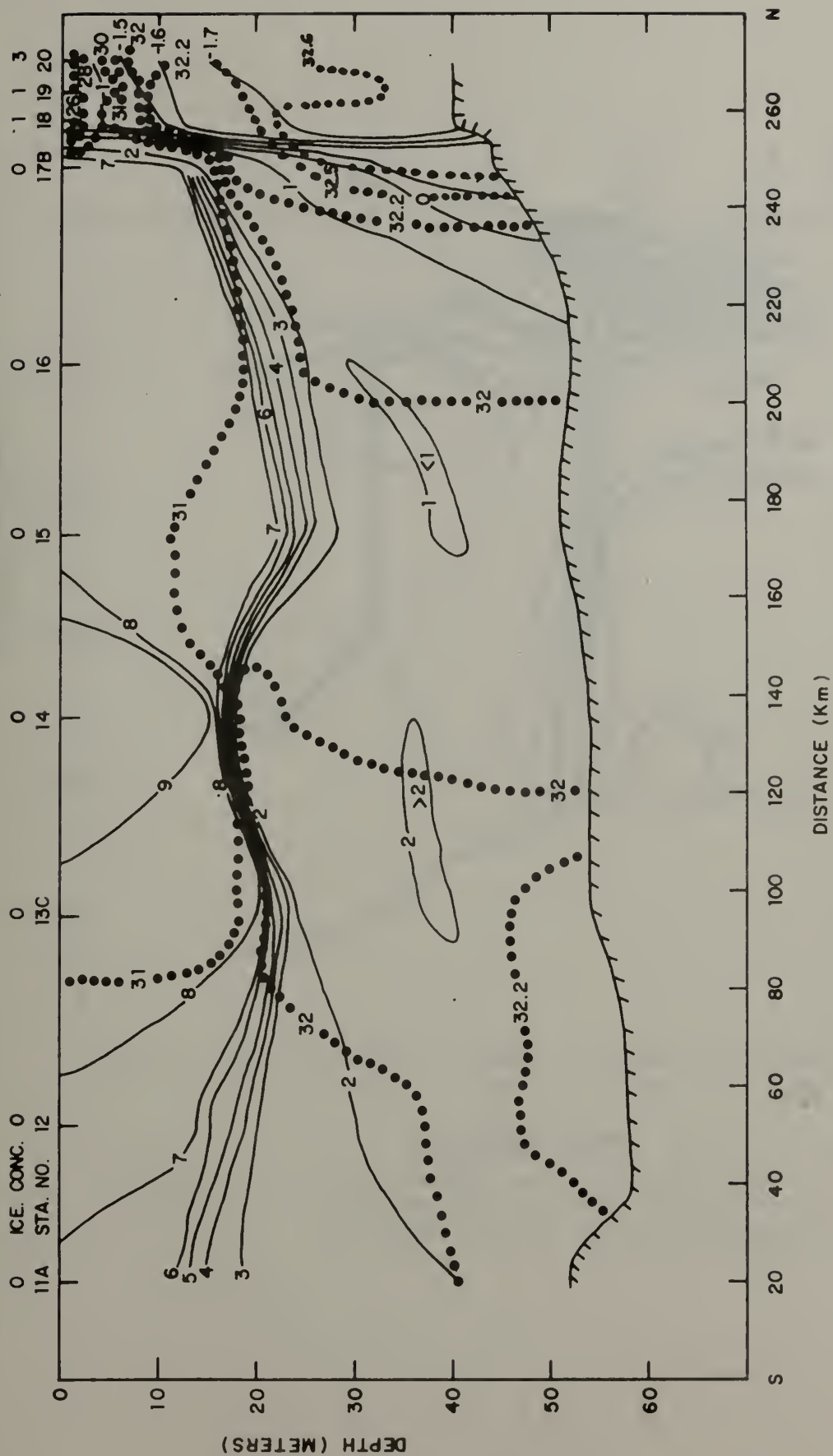


Figure 10. Temperature and salinity cross section No. 2. Ice concentrations are in oktas (eighths).



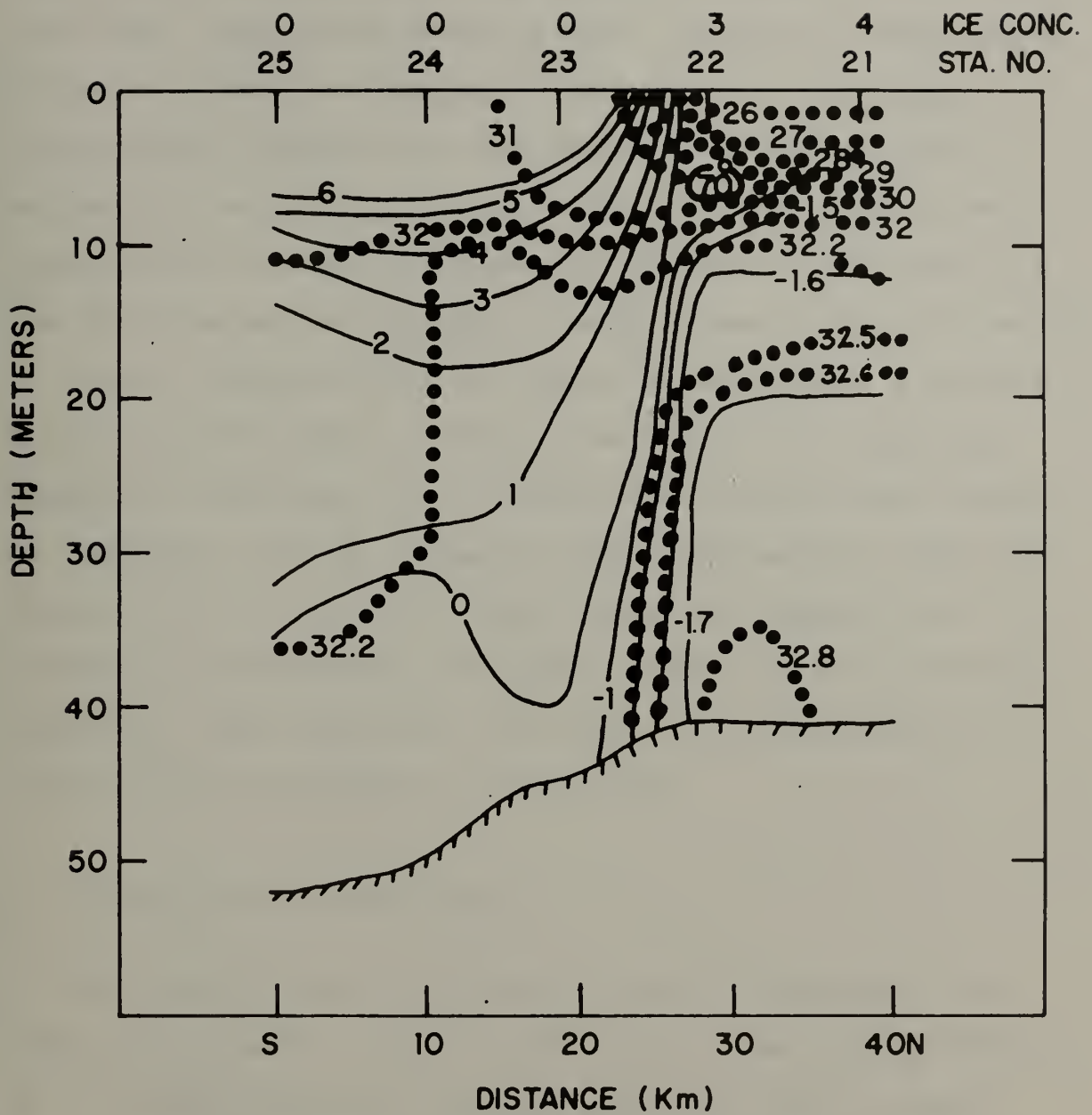


Figure 11. Temperature and salinity cross section No. 3. Ice concentrations are in oktas (eighths).





As would be expected from Graham's hypothesis (1978), little or no finestructure was found in association with this coincident temperature front in 1978. However, finestructure lenses were found at Stations 15 and 13C, 70 and 160 km, respectively, south of the ice edge. These examples are believed to be part of a large scale lateral mixing process. The low vertical salinity (density) gradient at the depth of the finestructure would tend to favor larger scale interleaving.

As was mentioned earlier, Figure 11 represents a revisit to a strong coincident front 12 hours later. The front has apparently maintained its intensity and location with respect to bathymetry, but by navigation the front and ice edge have moved a little south. The upper layer has thinned from 13 to 7 m and the thermocline has become considerably less intense. Seemingly, there has been a horizontal divergence near the surface and a convergence at mid-depths.

#### B. CROSS-SECTIONS NOS. 4 AND 5

The area depicted by Figures 12 and 13 represents the region of the most intense finestructure found during MIZPAC 78. The weak mid-depth salinity gradients found in these cross-sections contribute to the extensive interleaving. The complex nature of the flow regime in this area makes corroboration of previous theories difficult, i.e., the association of current patterns with finestructure and frontal formation. However, a few points are worth considering.



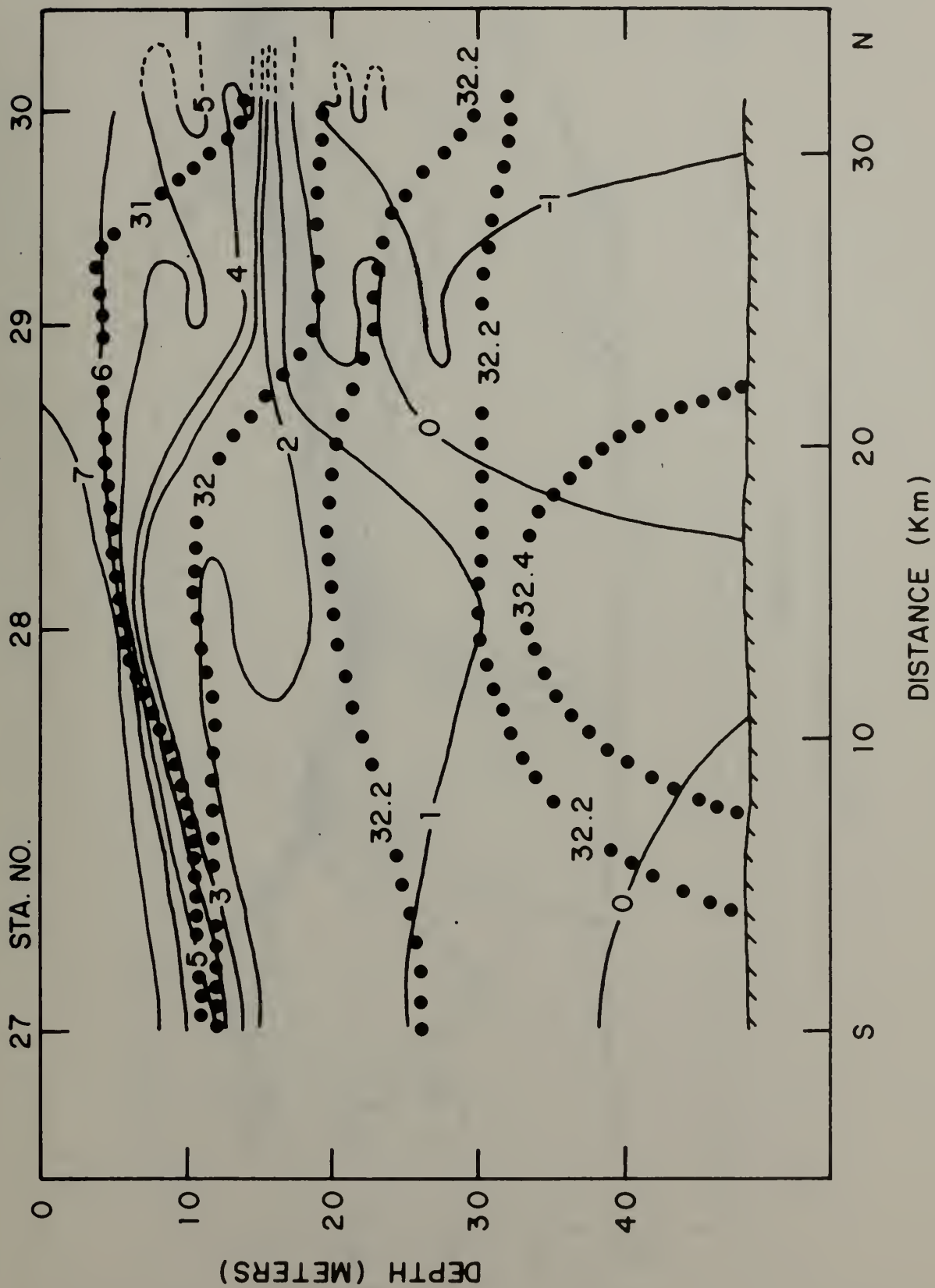


Figure 12. Temperature and salinity cross section No. 4.



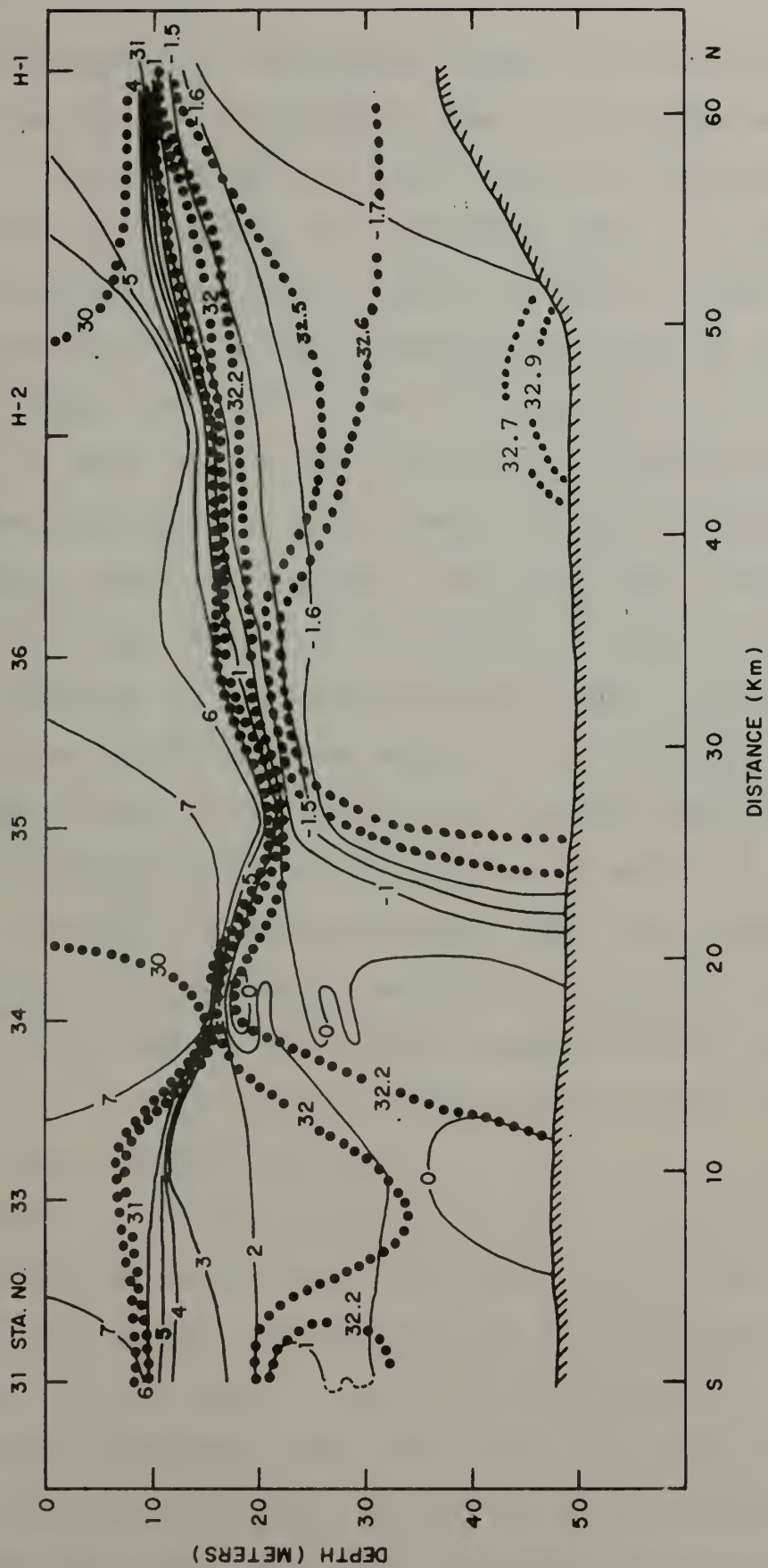


Figure 13. Temperature and salinity cross section  
No. 5.



Neither upper nor lower-layer fronts are seen in Figure 12 probably because of the distance from the ice edge and the failure to intersect either of the two basic water masses. This section is evidently in transition water. In Figure 13, which extends farther north, there is a front in the lower layer which involves northern bottom water only as cold as  $-1.6^{\circ}\text{C}$ . Again, the  $-1.7^{\circ}\text{C}$  water in Figure 13 has an associated salinity of  $32.6 \text{ }^{\circ}/\text{oo}$ , lower than the  $32.8 \text{ }^{\circ}/\text{oo}$  normally associated with northern bottom water. Some diluting process is assumed to have taken place. Note also that a wedge-like front is forming. Note also the pocket of high salinity water at the base of the slope in this figure. Evidently, a more saline northern bottom water exists in places. Probably it existed in many places earlier and has not been eroded or pushed back here because of the protective action of the slope. Presumably, a station farther north and closer to the ice edge would reveal characteristic northern bottom water. Cross-sections of stations occupied in the same general area in 1975 showed a similar lack of fronts but intense finestructure activity.

It should be noted that Stations 26, 28 and 34 are side by side, each approximately 10 km apart (Figure 14). These stations show marked finestructure of similar characteristics. Evidently, in this region, finestructure elements are at least 20 km in breadth, much longer than their intrusive length. Paquette and Bourke (1978c) reported a similar situation under almost identical ice edge/current conditions in MIZPAC 74.







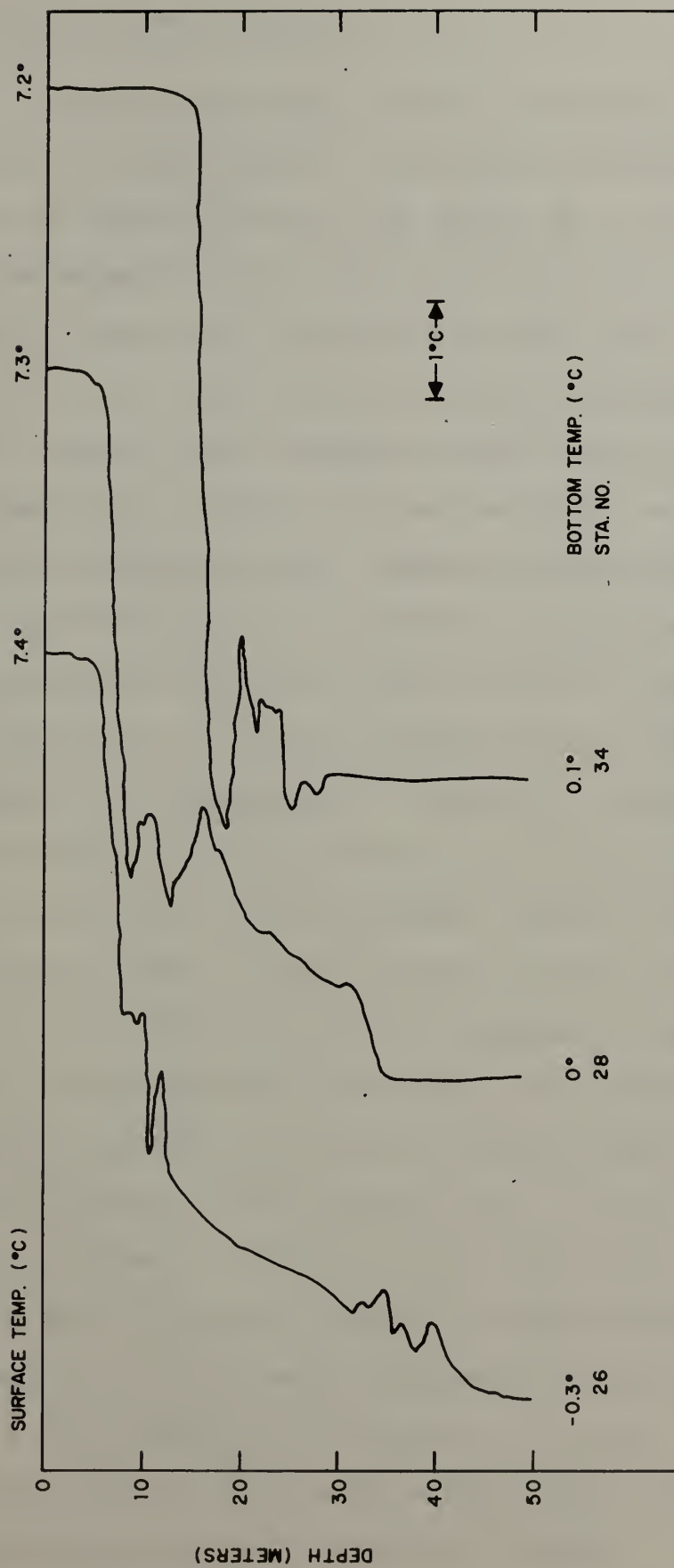


Figure 14. Nested temperature profile No. 3.



### C. THE WESTERN EMBAYMENT

A review of the shape of the ice edge during all MIZPAC cruises to date reveals a recurring ice embayment to the north of Cape Lisburne (see Figure 2). The consistency of this embayment's size and location and its value as an indicator of upper-level current flow have made it an object of extensive investigation in the MIZPAC program. In previous years stations were occupied around the periphery of this embayment and a number of cross-sections were taken normal to and into the ice edge. However, during MIZPAC 78, stations were occupied also in the center of the embayment to discover the phenomena associated with the core of warm surface flow.

The line of stations occupied through the center of the embayment is represented by Figure 15. A northern bottom water with a salinity of only 32.6 ‰ is evident in this cross-section at the northernmost station, H-14. This section is taken through the core of the jet-like current that is presumably causing the embayment and shows a continual supply of warm upper-layer water from the south. Only just south of Station H-14 does this water appear to show the cooling effects of the melting ice. It is assumed that this water continues to flow northward under the ice. The southern bottom water evidently extends up the embayment and pushes the northern bottom water northward so that it extends to only a few kilometers outside the ice edge. There is no extension, far to the south, of the lower layer front, as was suggested by Paquette and Bourke (1978c).



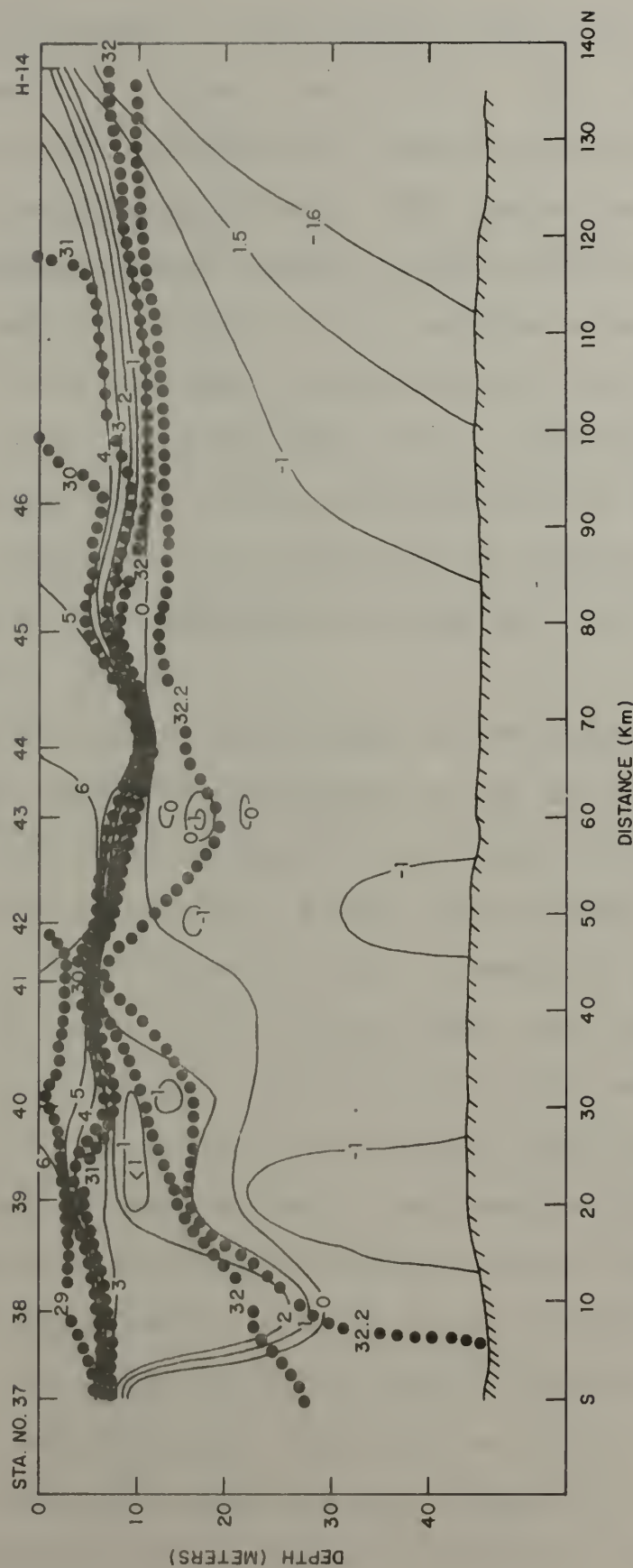


Figure 15. Temperature and salinity cross section No. 5A.



Figure 16 represents a cross-section across the west side of the embayment and its jet core current. The edge of northern bottom water is seen extending out from the ice at Station H-5 in the classic wedge-shaped front. The core of warm water flowing northward is again evident in this section as it is in Figures 17 and 18. Figure 17 is a section across the eastern half of the embayment, an extension of the crossing in Figure 16. The reason for the lack of a more distinguishable front in the lower layer of this cross-section is not clear but might be related to the tendency of the current to flow on the right side of the embayment and scour out the bottom water under the edge of the ice.

The extensive finestructure found in the southern and western portions of the embayment (see Figure 8) may be contrasted to the results reported by Zuberbuhler and Roeder (1976). Their measurements were taken mainly around the periphery of the embayment at or just inside the ice. It was only near the mouth of the bay and a little outside that they found notable finestructure. In similar locations our results would agree. The existence of finestructure in a region where strong horizontal fronts are absent indicates that near the sides of the embayment lateral mixing and intrusions must be occurring with northern bottom water, with the mixing strongest near the surface. The wedge-like front seen in Figure 16 is the result. One should note again that the low vertical salinity gradient is conducive to finestructure formation. It should be further noted that finestructure essentially disappears at Station 46 and farther north.





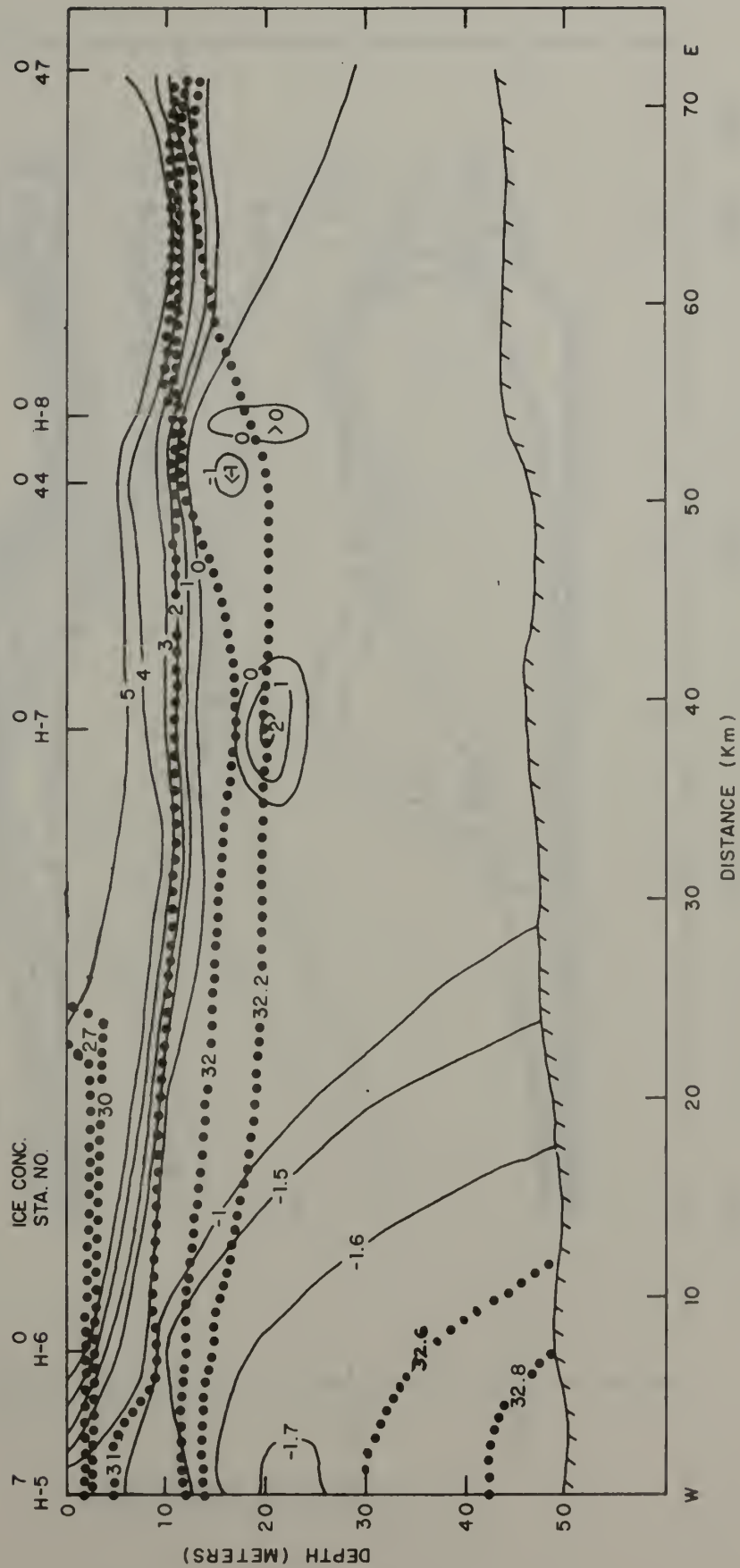


Figure 16. Temperature and salinity cross-section No. 6. Ice concentrations are in oktas (eighths). Temperatures are in degrees centigrade ( $^{\circ}\text{C}$ ). Salinities are in parts per thousand ( $\text{‰}$ ).



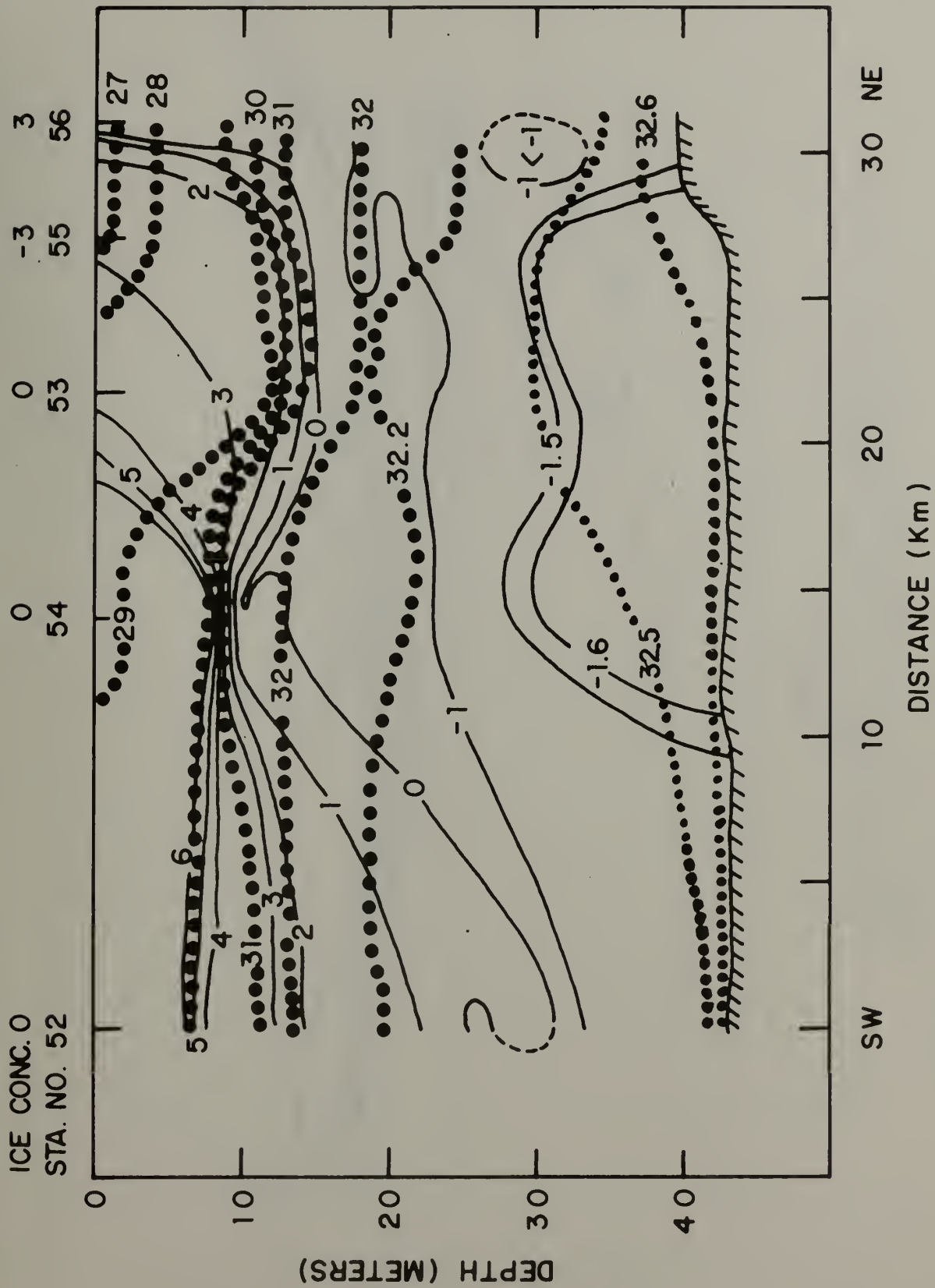


Figure 17. Temperatures and salinity cross-section No. 7. Ice concentrations are in oktas (eighths) except that a negative value, -b, indicates a concentration of 10-b.



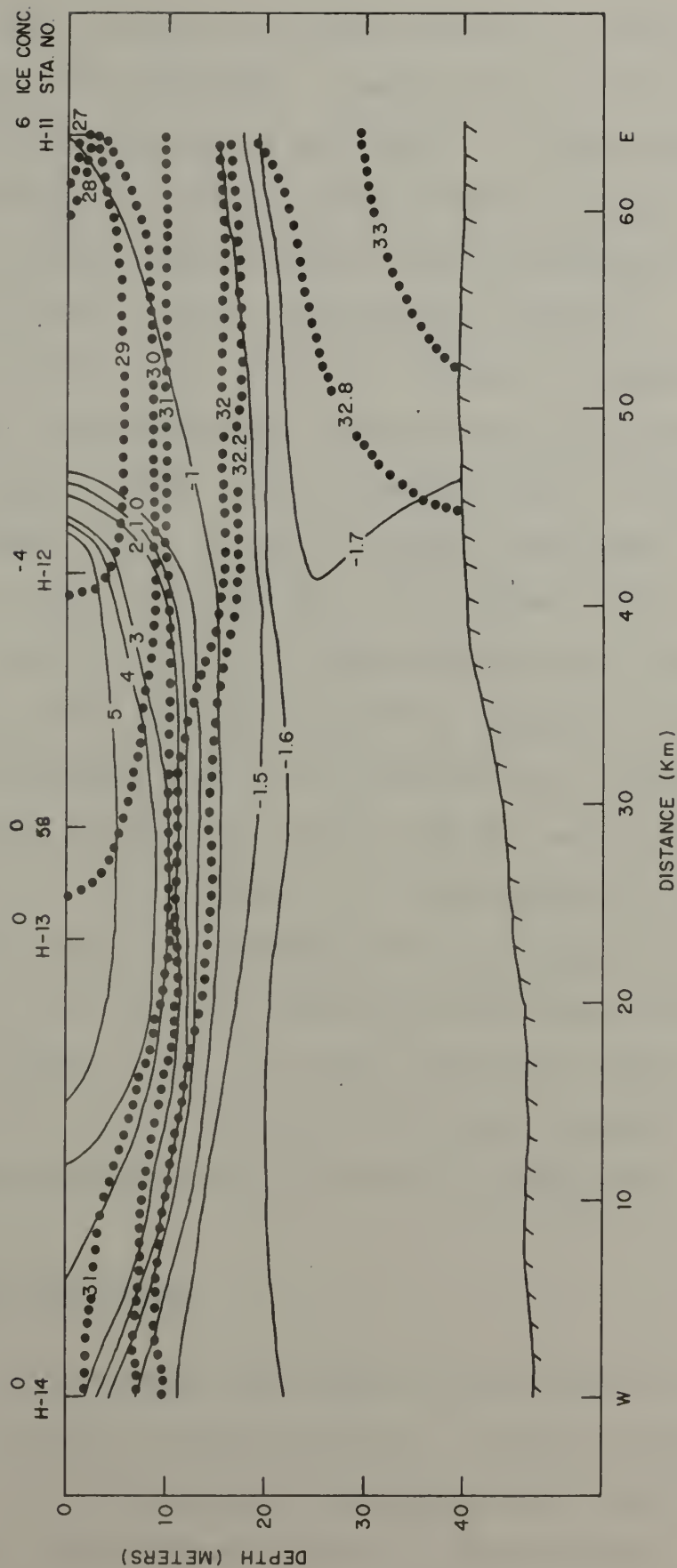


Figure 18. Temperature and salinity cross-section No. 8. Ice concentrations are in oktas (eighths) except that a negative value, -b, indicates a concentration of 10-b.



In contrast, little or no finestructure is found on the eastern side of the embayment, possibly due to the stronger vertical density gradient in mid-depth. By some extension of the definition, a weak coincident front is seen in Figure 17 at Station 56 which would indicate a mild shearing of water masses and an area of weak finestructure activity.

Further to the north, Figure 18 depicts a crossing of the eastern side of the embayment. Warm water on the surface is still strikingly evident and is centered well to the right of the embayment axis. There is a sharp coincident front essentially at the ice edge and, in agreement with Graham's hypothesis (1978), there is no finestructure near the front. It is not clear why the front should be sharper on the eastern side of the embayment than on the western side (Figure 16).

Considering the bottom contours and the warm cores from the temperature cross-sections, it would appear that the current which erodes the embayment had its origin from one of the branches of the current bifurcation off Cape Lisburne. The current appears to be initially steered by the trough on the western side of the embayment, but then crosses to the eastern side approximately halfway up the embayment.

#### D. THE BARROW EMBAYMENT

Another ice embayment was found during MIZPAC 78, this one to the northeast of Point Barrow. A similar embayment was found in the same general location in 1971, 1972 and 1977. As with the embayment north of Cape Lisburne, stations were occupied in the center of the embayment and the section







through these stations is shown in Figure 19. In this figure two warm cores may be seen. This evidence, together with the melt-back of the ice bay, indicates that the Alaskan Coastal Current apparently splits again off Point Barrow and causes this embayment. The case for bathymetric steering can again be made by examining Figure 19 and following the warm core and temperature maxima (Figure 20) along the 25-30 fm contour shown in Figure 9.

A sharp temperature and salinity front between the Alaskan Coastal Current and Chukchi Sea water is seen off the coast near Stations 75 and 76. This steepening of isopycnals along the shoreward canyon slope near Point Barrow may be seen in every available oceanographic section in the area. This is undoubtedly a geostrophic response to the strong Alaskan Coastal Current near shore. There is no finestructure associated with this front indicating little mixing between the two waters. The only evidence of strong finestructure activity in this embayment occurs at Stations 77 and 78. There is a noticeable cold, fresh spot at these stations with ice floes present. This is an extension of the ice projection to the north and provides further evidence of the current's control of ice melt patterns. It is likely that at Stations 77 and 78, the section crossed a frontal area with attendant finestructure which, farther to the northwest, extends along the ice edge and is thus removed from the cruise track. Unlike 1977 when extensive finestructure was found in this embayment, little was found during MIZPAC 78 probably due to







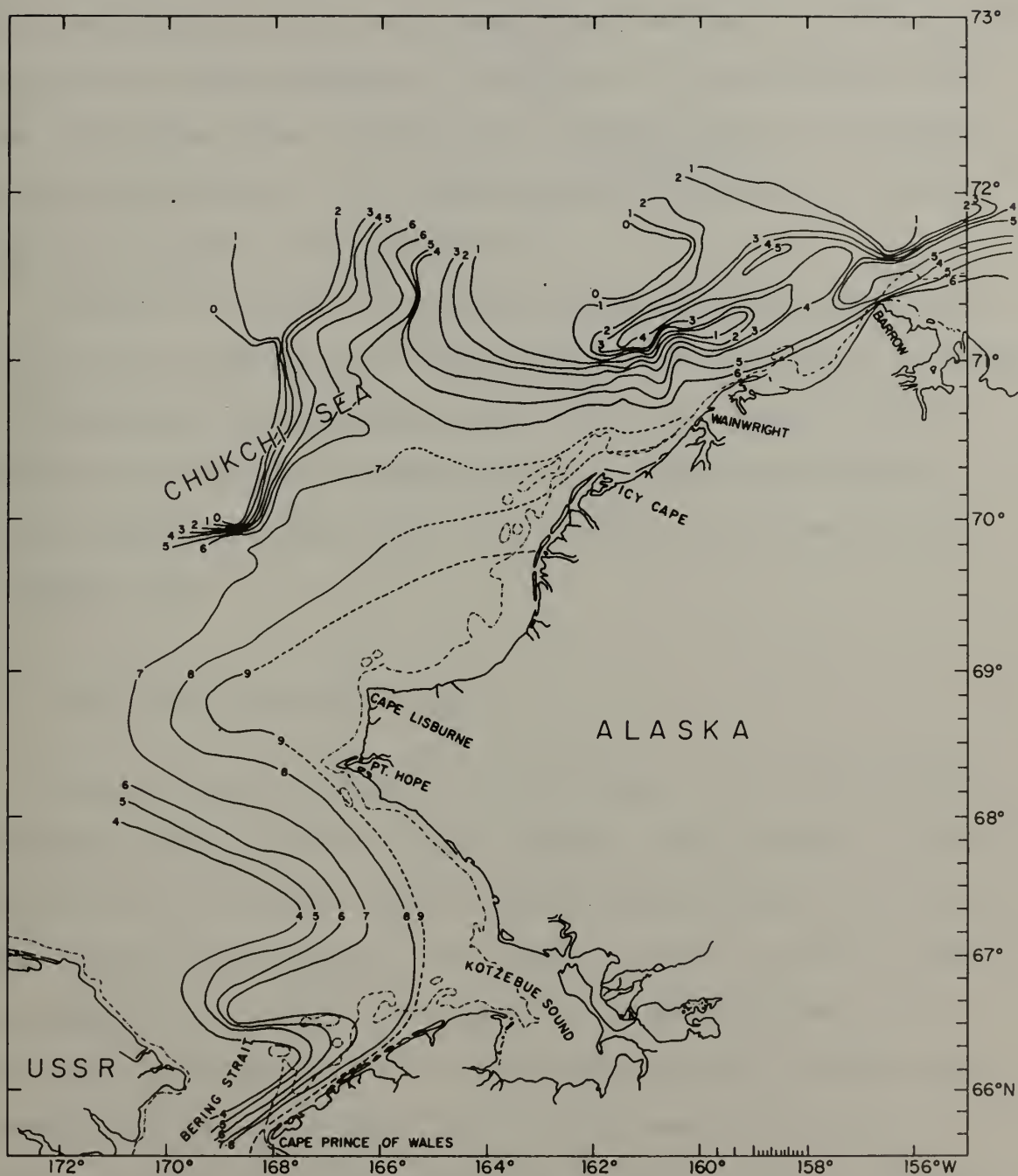


Figure 20. Isotherms of maximum temperature in the water column for MIZPAC 78. Temperatures are in degrees centigrade ( $^{\circ}\text{C}$ ). The dashed line paralleling the coast represents the 10 fathom curve.





the fact that the cruise track did not sample areas where finestructure is likely. It is presumed that more examples of finestructure would have been found had more stations been occupied in this embayment. The lack of finestructure near the end of the line (Station 85) is unexplained in contrast to the consistency of the finestructure intensity at similar stations occupied during MIZPAC 77.

Station 77 showed the deepest instance of finestructure ( $>90$  m) ever observed in MIZPAC data. The warm water involved in interleaving undoubtedly comes from the Alaskan Coastal Current which has here submerged to a considerable depth. Similar deep structure, but less intense, was found in 1977 (Graham, 1978).

#### E. CROSS-SECTIONS NOS. 9 AND 10

Cross-section 9 (Figure 21) is taken across the Alaskan Coastal Current north of Point Barrow. The current is quite narrow at the surface, being constrained between Point Barrow and the ice which usually lies close offshore in this region in summer. The northern boundary has submerged under the ice edge as it did in 1971; the seaward extent of this warm current is seen in Figure 22. A coincident-type front is seen in Figure 21 between Stations 66 and 67 and the seaward breakdown of this front is seen in Figure 22. As was anticipated, little finestructure was found in the vicinity of the coincident front, but very intense structure was found farther to the northeast (Station 60) as the Alaskan Coastal Current plunged into the Beaufort Sea.





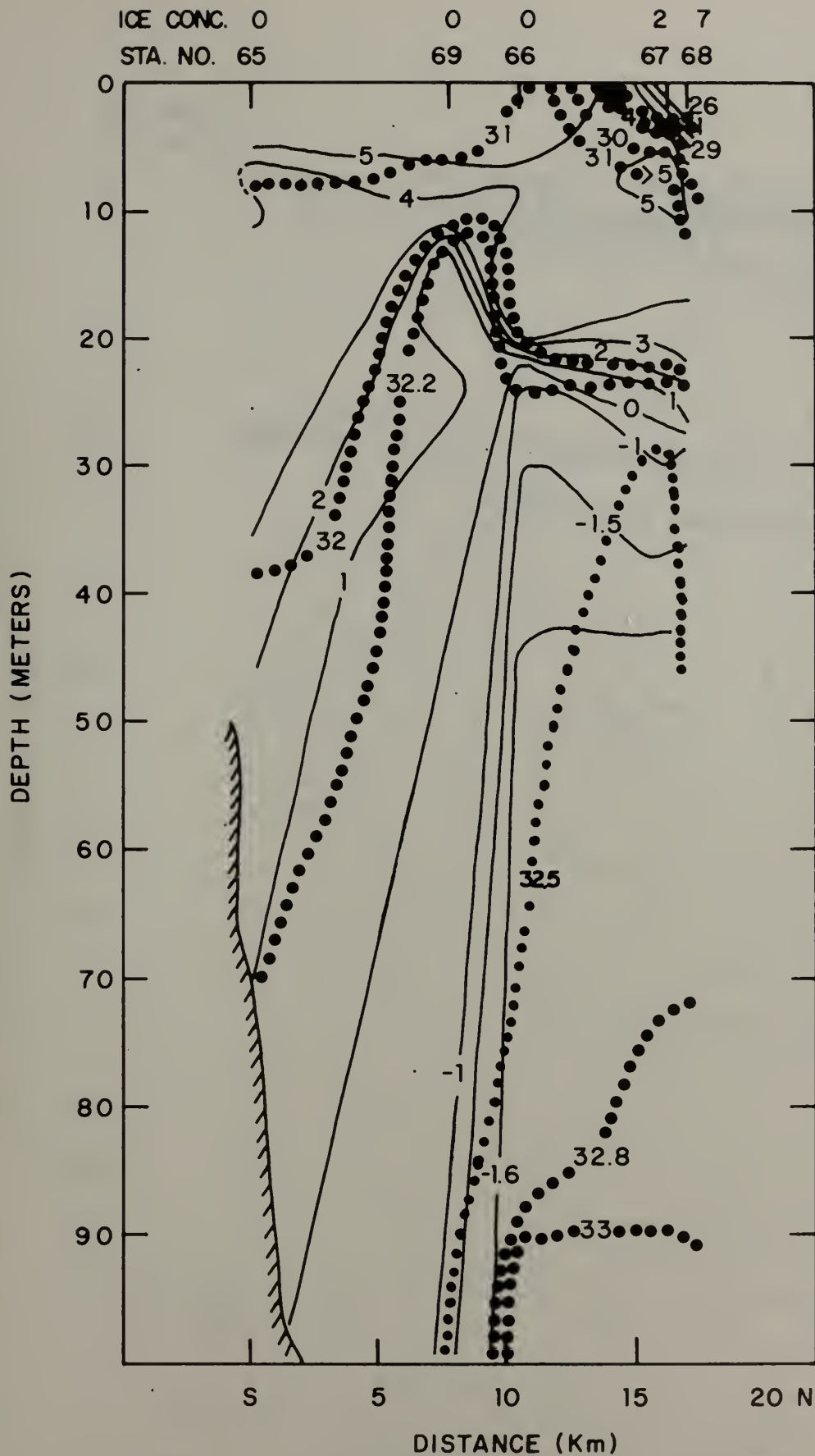


Figure 21. Temperature and salinity cross section No. 9. Ice concentrations are in oktas (eighths). Temperatures are in degrees centigrade ( $^{\circ}\text{C}$ ). Salinities are in parts per thousand ( $^{\circ}/_{\text{oo}}$ ).



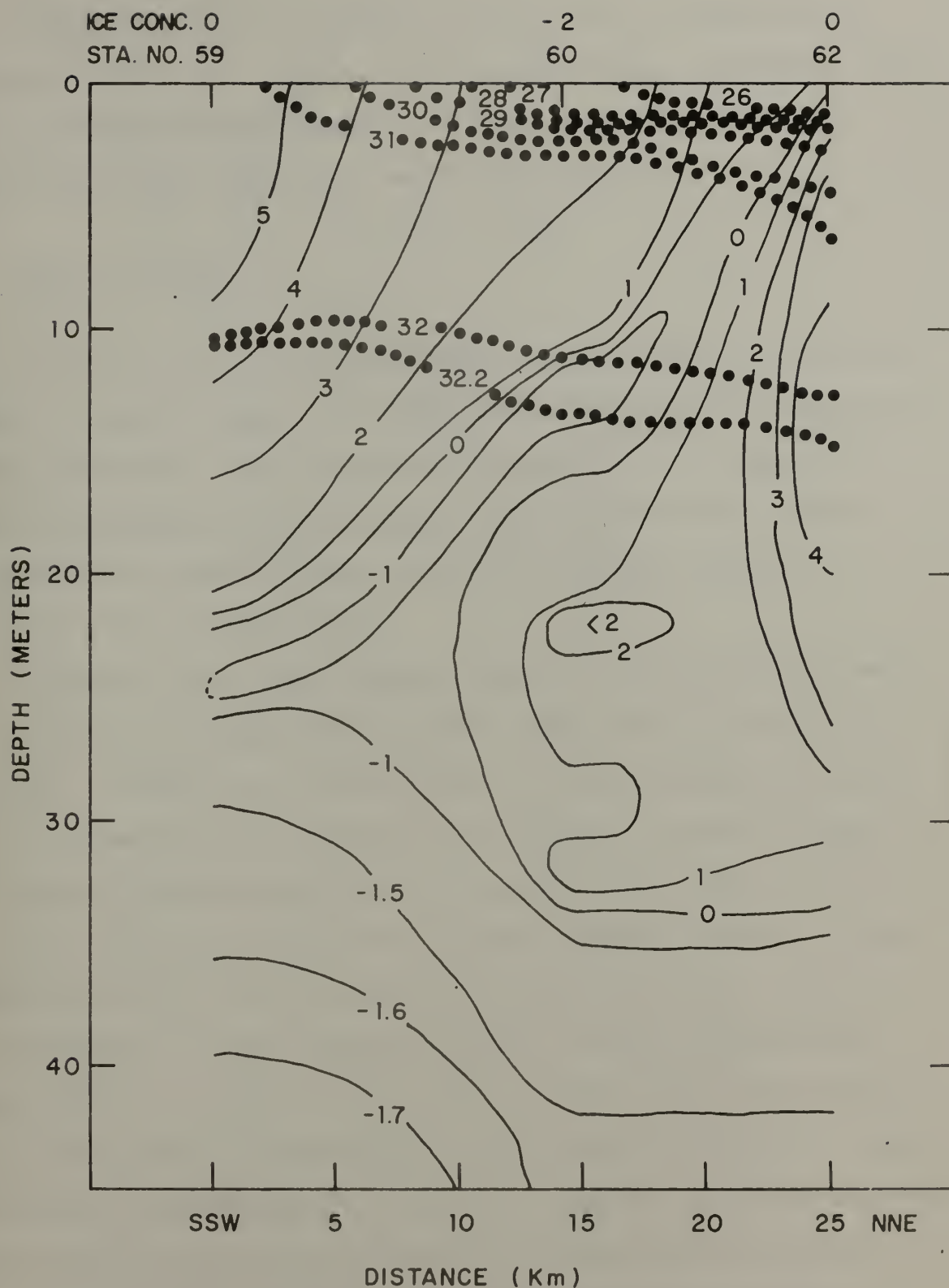


Figure 22. Temperature and salinity cross section No. 10. Ice concentrations are in oktas (eighths) except negative values,  $-b$ , which represent concentrations of  $10^{-b}$ .



Finestructure with depths up to 90 m was found in this region (Figure 22). Again, this finestructure originates from the submerged Alaskan Coastal Current or some finger-like extension of its relatively warm ( $4^{\circ}\text{C}$ ) water.

#### F. THE ICE "TONGUE"

A peculiar ice tongue was found south of the Barrow embayment; a similar tongue was found in the same relative location during MIZPAC 77 and reported by Graham (1978). Figures 23 and 24 represent sections across and into the tip of this tongue while Figure 25 cuts across the Alaskan Coastal Current south of the tongue.

Figure 23 shows very dense northern bottom water trapped in a 25-30 fm trough beneath and to the south of the ice tongue. A sharp lower-layer front is seen beneath Station 91. Its termination might be due to an apparent clockwise gyre at depth as indicated by the rising  $32.8$  ‰ isohaline or to the shearing effect of the Alaskan Coastal Current. This shearing effect is better seen in Figure 25 which indicates a bifurcation of the Alaskan Coastal Current with the warm core ( $6^{\circ}\text{C}$ ) to the east but another slightly cooler and deeper core ( $4^{\circ}\text{C}$  and 20 m) passing through Stations 91 and 92. This bifurcated branch appears to be following the 25-30 fm contour (see Figure 9) and causing the small depression in the ice edge south of the tongue. The warm water of this branch is seen flowing under the ice at Station H-19. The most intense finestructure in this area was found at this point where the



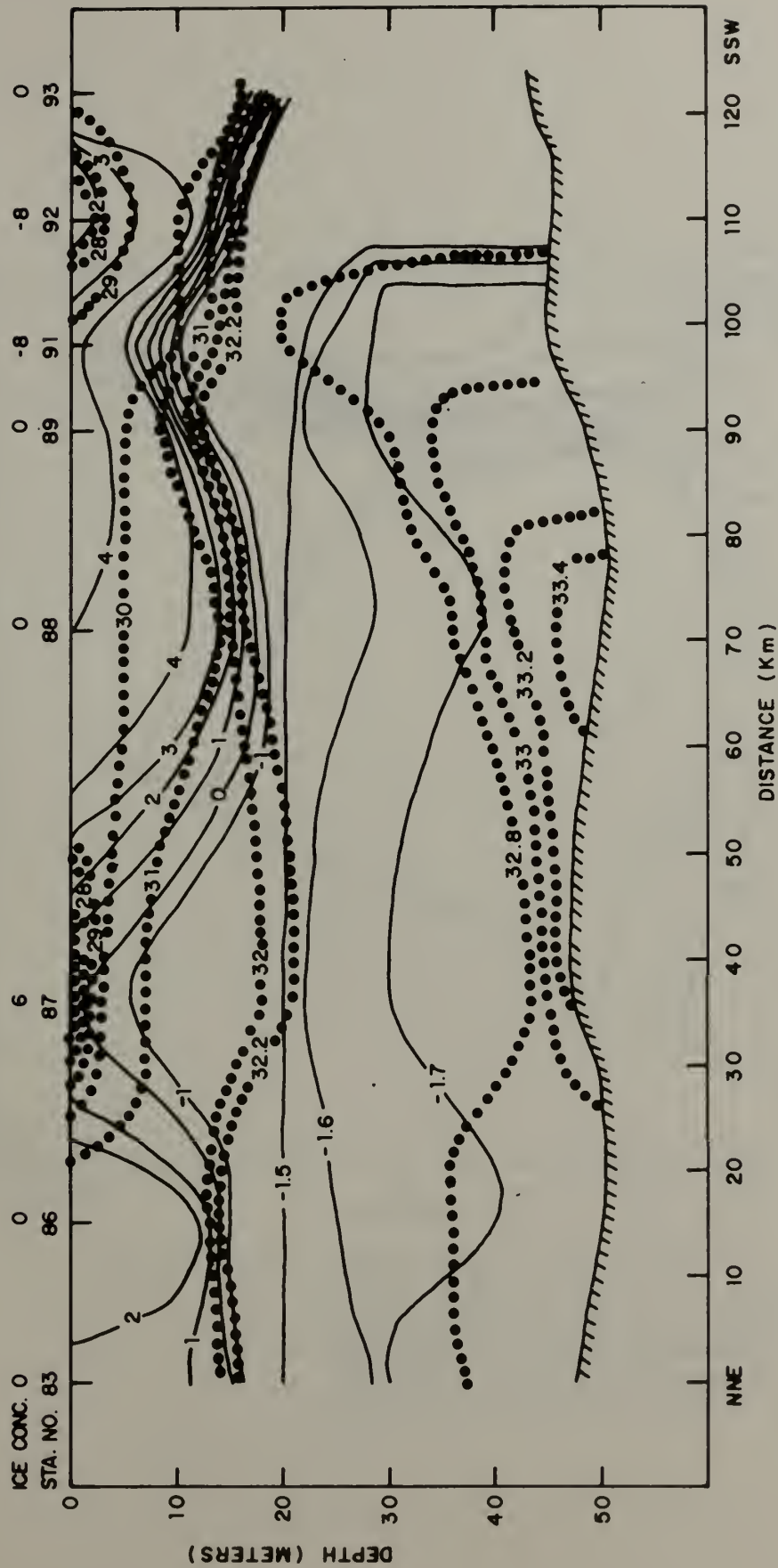
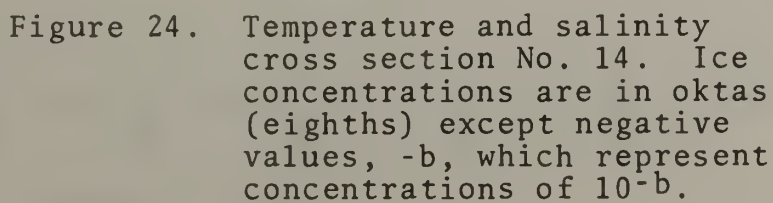


Figure 23. Temperature and salinity cross-section No. 12.  
Ice concentrations are in oktas (eighths)  
except negative values, -b, which indicate  
concentrations of 10-b.













lower-layer front appears in the classic wedge-shape form conducive to finestructure formation.

Figure 24 shows a cross-section into the tip of the ice tongue. Its forwardmost protrusion would indicate an area of slow ice edge recession and the moderate coincident front seen under Station 104 comes as no surprise. Only weak finestructure was found in this vicinity which would be expected upon examination of the strong, mid-depth salinity gradients. This frontal location and relative lack of finestructure in an area of slow ice edge recession is in agreement with the findings earlier in the cruise and the predictions of Graham (1978) and Paquette and Bourke (1978b and c).





## VI. CONCLUSIONS

Data gathered during the MIZPAC 78 cruise to the Chukchi Sea were displayed and analyzed with special attention being paid to finestructure, fronts, and upper level currents. The phenomena observed in 1978 were compared with those seen in previous cruises and the following conclusions resulted:

- Several hypotheses arising from previous MIZPAC cruises were tested and the MIZPAC 78 data were found to be in agreement with these predictions. Specifically, strong coincident temperature fronts with little associated finestructure were found to exist in regions of bifurcation of upper-level currents where there is little or no component of flow toward the ice edge. Further, the upper-level currents as inferred from ice edge recession rates from 14 to 28 July 1978 conformed to previously postulated patterns.
- Upper level currents, as inferred from ice edge recession rates, temperature cross-sections, and water column temperature maxima were examined with respect to the bottom bathymetry and were found to flow roughly parallel to the bottom contours. Specifically, the bifurcation of the water flowing through the Bering Strait, the warm core jets



causing the two ice embayments, and the minor split of the Alaskan Coastal Current causing the indentation in the Barrow ice tongue were found to conform to the concept of bathymetric steering.

- An embayment north of Cape Lisburne was the object of the most extensive examination of ice embayments to date. The embayment was found to exhibit considerable consistency with respect to size and location over a series of six MIZPAC cruises. The center of the embayment was examined and found to be an area of extensive finestructure activity. The absence of a sharp lower-layer front was attributed to the strong flow of southern water which had apparently pushed the northern bottom water beyond any of the stations occupied.

- The ice embayment northwest of Point Barrow was examined in a manner similar to the one north of Cape Lisburne. Although little finestructure was found, it was presumed that the cruise track did not sample regions where intense finestructure activity could be expected. The deepest finestructure found to date was found in this embayment and the waters involved in the interleaving were associated with the submergence of the warm Alaskan Coastal Current.



## LIST OF REFERENCES

- Bourke, R. H. and R. G. Paquette, 1976, Atlantic Water on the Chukchi Shelf, Geophys. Res. Lett., 3(10):629-632.
- Bourke, R. H. and R. G. Paquette, 1977, Low-Frequency Acoustic Propagation and Oceanography of the Pacific Marginal Sea Ice Zone, U.S. Navy J. Underwater Acoustics, 27(1):191-209.
- Coachman, L. K., K. Aagaard, R. B. Tripp, 1975, Bering Strait: The Regional Physical Oceanography, Univ. of Washington Press, Seattle, 172 pp.
- Corse, W. R., 1974, An Oceanographic Investigation of Mesos-structure Near Arctic Ice Margins, Master's Thesis, Naval Postgraduate School, Monterey.
- Garrison, G. R., E. A. Pence, H. R. Feldman, S. R. Shah, 1974, Studies in the Marginal Ice Zone of the Chukchi Sea: Analysis of 1972 data, APL-UW 7311 Applied Physics Lab., Univ. of Washington, Seattle.
- Garrison, G. R. and P. Becker, 1975, Marginal Sea Ice Zone Oceanographic Measurements: Bering and Chukchi Seas, 1973 and 1974, APL-UW 7505, Applied Physics Lab., Univ. of Washington, Seattle.
- Goodman, J. R., J. H. Lincoln, T. G. Thompson, F. A. Zeusler, 1942, Physical and Chemical Investigations: Bering Sea, Bering Strait, Chukchi Sea During the Summers of 1937 and 1938, Univ. of Washington Press, Seattle.
- Graham, G. P., 1978, Finestructure, Fronts and Currents in the Pacific Marginal Sea-Ice Zone - MIZPAC 77, Master's Thesis, Naval Postgraduate School, Monterey, Tech. Rpt. No. NPS 68-78-006.
- Handlers, R. G., 1977, On the Question of Accumulation of Ice Melt Water South of the Ice in the Chukchi Sea, Master's Thesis, Naval Postgraduate School, Monterey, Tech. Rpt. No. NPS-68PA77031.
- Karrer, A. G., 1975, The Descriptive and Dynamic Oceanography of the Mesos-structure Near Arctic Ice Margins, Master's Thesis, Naval Postgraduate School, Monterey.
- Johnson, E. R., 1978, Quasigeostrophic Flow Above Sloping Boundaries, Deep Sea Res., 25(11):1049-1071.





- Paquette, R. G. and R. H. Bourke, 1973, Oceanographic Measurements Near the Arctic Ice Margins, Tech. Rpt. NPS-58PA 73121A, Dept of Oceanography, Naval Postgraduate School, Monterey.
- Paquette, R. G and R. H. Bourke, 1974, Observation of the Coastal Current of Arctic Alaska, J. Mar. Res., 32(2):195-207.
- Paquette, R. G. and R. H. Bourke, 1976, Oceanographic Investigations of the Marginal Sea-Ice Zone of the Chukchi Sea - MIZPAC 1974, Tech. Rpt. NPS-58PA76051, Dept. of Oceanography, Naval Postgraduate School, Monterey.
- Paquette, R. G. and R. H. Bourke, 1978a, The Oceanographic Cruise of the USCGC BURTON ISLAND to the Marginal Sea Ice Zone of the Chukchi Sea, Tech. Rpt. NPS 68-78-001, Dept. of Oceanography, Naval Postgraduate School, Monterey.
- Paquette, R. G. and R. H. Bourke, 1978b, Temperature Fine Structure Near the Sea-Ice Margin of the Chukchi Sea, J. Geophys. Res., 84(C3):1155-1165.
- Paquette, R. G. and R. H. Bourke, 1978c, Temperature Fronts in the Marginal Sea-Ice Zone of the Chukchi Sea, Paper Presented at the 1978 Fall Annual Meeting of the AGU, Abstract in: EOS, Trans., Am. Geophys. Un., 59(12):1091-1092.
- U.S. Navy Hydrographic Office, 1952, A Functional Glossary of Ice Terminology, H.O. Pub. No. 609, 88 pp.
- U.S. Navy Weather Service, 1976, Eastern-Western Arctic Sea-Ice Analysis, Fleet Weather Facility, Suitland, Maryland, 100 pp.
- U.S. Oceanographic Office, Oceanographic Atlas of the Polar Seas, Part III, Arctic, H. O. Pub. No. 705, 1958.
- Zuberbuhler, W. J. and J. A. Roeder, 1976, Oceanography, Mesosstructure and Currents of the Pacific Marginal Sea-Ice Zone - MIZPAC 75, Master's Thesis, Naval Postgraduate School, Monterey, Tech. Rpt. NPS-58PA76091.





# INITIAL DISTRIBUTION LIST

	No. Copies
1. Director Applied Physics Laboratory University of Washington 1013 Northeast 40th Street Seattle, Washington 98195	
Mr. Robert E. Francois	1
Mr. E. A. Pence	1
Mr. G. R. Garrison	1
Library	1
2. Director	25
Arctic Submarine Laboratory Code 54, Building 371 Naval Ocean Systems Center San Diego, California 92152	
3. Superintendent Naval Postgraduate School Monterey, California 93940	
Library, Code 0142	2
Dr. R. G. Paquette Code 68Pa	5
Dr. R. H. Bourke Code 68Bf	5
4. Polar Research Laboratory, Inc. 123 Santa Barbara Street Santa Barbara, California 93101	2
5. Chief of Naval Operations Department of the Navy Washington, D. C. 20350	
NOP-02	1
NOP-22	1
NOP-946D2	1
NOP-095	1
NOP-098	1
6. Commander	1
Submarine Squadron THREE Fleet Station Post Office San Diego, California 92132	
7. Commander	1
Submarine Group FIVE Fleet Station Post Office San Diego, California 92132	



8.	Director Marine Physical Laboratory Scripps Institution of Oceanography San Diego, California 92132	1
9.	Commanding Officer Naval Intelligence Support Center 4301 Suitland Road Washington, D. C. 20390	1
10.	Commander Naval Electronic Systems Command  Department of the Navy Washington, D. C. 20360 NESC 03 PME 124	1   1 1
11.	Director Woods Hole Oceanographic Institution Woods Hole, Massachusetts 02543	1
12.	Commanding Officer Naval Coastal Systems Laboratory Panama City, Florida 32401	1
13.	Commanding Officer Naval Submarine School Box 700, Naval Submarine Base, New London Groton, Connecticut 06340	1
14.	Assistant Secretary of the Navy (Research and Development) Department of the Navy Washington, D. C. 20350	2
15.	Director of Defense Research and Engineering Office of Assistant Director (Ocean Control) The Pentagon Washington, D. C. 20301	1
16.	Commander, Naval Sea Systems Command  Department of the Navy Washington, D. C. 20362	4
17.	Chief of Naval Research Department of the Navy 800 North Quincy Street Arlington, Virginia 22217 Code 102-OS Code 220 Code 461	1   1 1 1



18. Project Manager 1  
Anti-Submarine Warfare Systems Project  
Office (PM4)  
Department of the Navy  
Washington, D. C. 20360
19. Commanding Officer 1  
Naval Underwater Systems Center  
Newport, Rhode Island 02840
20. Commander 2  
Naval Air Systems Command  
Headquarters  
Department of the Navy  
Washington, D. C. 20361
21. Commander 2  
Naval Oceanographic Office  
Washington, D. C. 20373  
Attention: Library Code 3330
22. 2  
  
Defense Documentation Center  
Cameron Station  
Alexandria, Virginia 22314
23. Director 1  
Advanced Research Project Agency  
1400 Wilson Boulevard  
Arlington, Virginia 22209
24. Commander SECOND Fleet 1  
Fleet Post Office  
New York, New York 09501
25. Commander THIRD Fleet 1  
Fleet Post Office  
San Francisco, California 96601
26. Commander  
Naval Surface Weapons Center  
White Oak  
Silver Spring, Maryland 20910  
Mr. M. M. Kleinerman 1  
Library 1
27. Officer-in-Charge 1  
New London Laboratory  
Naval Underwater Systems Center  
New London, Connecticut 06320





28.	Commander Submarine Development Group TWO Box 70 Naval Submarine Base New London Groton, Connecticut 06340	1
29.	Commander Naval Weapons Center China Lake, California 93555 Attention: Library	1
30.	Commander Naval Electronics Laboratory Center 271 Catalina Boulevard San Diego, California 92152 Attention: Library	1
31.	Director Naval Research Laboratory Washington, D. C. 20375 Attention: Technical Information Division	3
32.	Director Ordnance Research Laboratory Pennsylvania State University State College, Pennsylvania 16801	1
33.	Commander Submarine Force U. S. Atlantic Fleet Norfolk, Virginia 23511	1
34.	Commander Submarine Force U. S. Pacific Fleet N-21 Pearl Harbor, Hawaii 96860	1
35.	Commander Naval Air Development Center Warminster, Pennsylvania 18974	1
36.	Commander Naval Ship Research and Development Center Bethesda, Maryland 20084	1
37.	Chief of Naval Material Department of the Navy Washington, D. C. 20360 NMAT 03 NMAT 034 NMAT 0345	2 1 1



38. Commandant 2  
U. S. Coast Guard Headquarters  
400 Seventh Street, S.W.  
Washington, D. C. 20590
39. Commander 1  
Pacific Area, U. S. Coast Guard  
630 Sansome Street  
San Francisco, California 94126
40. Commander 1  
Atlantic Area, U. S. Coast Guard  
Governors Island  
New York, New York 10004
41. Commanding Officer  
U. S. Coast Guard Oceanographic Unit  
Building 159E, Navy Yard Annex  
Washington, D. C. 20590  
Dr. D. G. Mountain 1
42. Department of Oceanography, Code 68 3  
Naval Postgraduate School  
Monterey, California 93940
43. Oceanographer of the Navy 1  
Naval Oceanography Division (OP 952)  
Navy Department  
Washington, DC 20350
44. Office of Naval Research, Code 410 1  
NORDA, NSTL  
Bay St. Louis- Mississippi 39520
45. Dr. Robert E. Stevenson 1  
Scientific Liaison Office, ONR  
Scripps Institution of Oceanography  
La Jolla, California 92037
46. SIO Library 1  
University of California, San Diego  
P. O. Box 2367  
La Jolla, California 92037
47. University of Washington  
Seattle, Washington 98105  
Dept. of Oceanography Library 1  
Dr. L. K. Coachman 1
48. Department of Oceanography Library 1  
Oregon State University  
Corvallis, Oregon 97331



49. Commanding Officer 1  
Fleet Numerical Weather Central  
Monterey, California 93940
50. Commanding Officer 1  
Naval Environmental Prediction Research  
Facility  
Monterey, California 93940
51. Director 1  
Naval Arctic Research Laboratory  
Barrow, Alaska 99723  
Library
52. Department of the Navy 1  
Commander Oceanographic System Pacific  
Box 1390  
Pearl Harbor, Hawaii 96860
53. Commander 1  
Naval Oceanography Command  
National Space Technology Laboratories  
Bay St. Louis, Mississippi 39529
54. NORDA 1  
Technical Director  
Bay St. Louis, Mississippi 39520
55. Department of Meteorology Library 1  
Naval Postgraduate School, Code 63  
Monterey, California 93940
56. LCDR Gordon P. Graham 1  
Canadian Forces Fleet School  
Halifax, Nova Scotia  
Canada, B3K 2X0
57. CDR William J. Zuberbuhler 1  
Commanding Officer  
Naval Facility  
Lewes, Delaware 19958
58. LCDR Warren E. Small 1  
COMCARGRU THREE Staff  
FPO San Francisco, California 96601
59. LT Walter R. Lohrmann 1  
SWOSCOLCOM  
Newport, Rhode Island 02840



182133

Thesis  
S57184  
c.1

Small

Finestructure,  
fronts and currents  
in the Pacific mar-  
ginal sea-ice zone -  
MIZPAC 78.

132133

Thesis  
S57184  
c.1

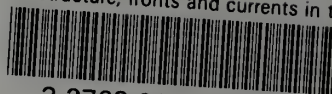
Small

Finestructure,  
fronts and currents  
in the Pacific mar-  
ginal sea-ice zone -  
MIZPAC 78.



thesS57184

Finestructure, fronts and currents in th



3 2768 002 00864 1

DUDLEY KNOX LIBRARY